

Soft photons in hadron-hadron collisions: synchrotron radiation from the QCD vacuum?

G.W. Botz, P. Haberl, O. Nachtmann

Institut für Theoretische Physik, Universität Heidelberg, Philosophenweg 16, D-69120 Heidelberg, Germany

Received: 27 October 1994

Abstract. We discuss the production of soft photons in high energy hadron-hadron collisions. We present a model where quarks and antiquarks in the hadrons emit “synchrotron light” when being deflected by the chromomagnetic fields of the QCD vacuum, which we assume to have a nonperturbative structure. This gives a source of prompt soft photons with frequencies $\omega \lesssim 300$ MeV in the c.m. system of the collision in addition to hadronic bremsstrahlung. In comparing the frequency spectrum and rate of “synchrotron” photons to experimental results we find some supporting evidence for their existence. We make an exclusive–inclusive connection argument to deduce from the “synchrotron” effect a behaviour of the neutron electric formfactor $G_E^n(Q^2)$ proportional to $(Q^2)^{1/6}$ for $Q^2 \lesssim 20 \text{ fm}^{-2}$. We find this to be consistent with available data. In our view, soft photon production in high energy hadron-hadron and lepton-hadron collisions as well as the behaviour of electromagnetic hadron formfactors for low Q^2 are thus sensitive probes of the nonperturbative structure of the QCD vacuum.

1 Introduction

According to current theoretical ideas the vacuum state of quantum chromodynamics (QCD) has a rich structure: it is characterized by various condensates of quarks and gluons. We shall study here possible effects of the gluon condensate in high energy hadron-hadron collisions: the emission of soft prompt photons in addition to photons from hadronic bremsstrahlung. For frequency $\omega \rightarrow 0$ the bremsstrahlung photons must dominate over photons from any other source due to Low’s theorem [1] which, in essence is just a consequence of electromagnetic gauge invariance. The occurrence of additional soft prompt photons with frequencies $\omega \lesssim 300$ MeV was predicted in [2]. There the following physical picture was developed: When quarks (q) and antiquarks (\bar{q}) of a fast hadron move through the QCD vacuum they are subjected to the chromoelectric and chromomagnetic vacuum fields. The

chromomagnetic Lorentz force will cause deflections of q and \bar{q} , will make them wiggle around a bit. Since q and \bar{q} carry electric charge, they will then emit synchrotron radiation. For a single hadron these synchrotron photons are part of the photon cloud around the hadron. But in a high energy hadron-hadron, lepton-hadron, or photon-hadron collision the photons can be set free, manifesting themselves as prompt photons with the characteristic energy spectrum of synchrotron radiation.

In this paper we will elaborate on the above idea. We will compare the predictions of our synchrotron effect with recent experimental results on soft photon production, especially the results of [3]. We will also make a duality argument to relate the synchrotron effect to the behaviour of the electromagnetic formfactors of hadrons as function of the momentum transfer squared Q^2 .

2 Synchrotron radiation from the QCD vacuum

The idea that there may be nonvanishing colour fields in the vacuum of QCD has a long history [4–10] (for recent reviews cf. [11, 12]). One important quantity characterizing the vacuum of QCD is the gluon condensate introduced in [5, 7]: There is ample phenomenological evidence that the product of two gluon field strengths at the same space-time point has a nonvanishing vacuum expectation value:

$$\begin{aligned}
 G_2 &:= \left\langle 0 \left| \frac{g^2}{4\pi^2} G_{\mu\nu}^a(x) G^{a\mu\nu}(x) \right| 0 \right\rangle \\
 &= \frac{1}{4\pi^2} (0.95 \pm 0.45) \text{ GeV}^4.
 \end{aligned} \tag{2.1}$$

Here and in the following we always work in Minkowski space; $G_{\mu\nu}^a(x)$ is the gluon field strength tensor with Lorentz indices μ, ν and colour index a ($a = 1, \dots, 8$) and g is the QCD coupling constant. All our notation follows [13]. The numerical value for G_2 is as quoted in [12]. Considering the uncontracted product of two field

strength tensors and using Lorentz and parity invariance one finds

$$\left\langle 0 \left| \frac{g^2}{4\pi^2} G_{\mu\nu}^a(x) G_{\rho\sigma}^b(x) \right| 0 \right\rangle = \frac{1}{96} \delta^{ab} (g_{\mu\rho} g_{\nu\sigma} - g_{\mu\sigma} g_{\nu\rho}) G_2. \quad (2.2)$$

For the chromoelectric and chromomagnetic fields this implies:

$$\begin{aligned} \langle 0 | g^2 \mathbf{B}^a(x) \mathbf{B}^a(x) | 0 \rangle &= \pi^2 G_2 \simeq (700 \text{ MeV})^4, \\ \langle 0 | g^2 \mathbf{E}^a(x) \mathbf{E}^a(x) | 0 \rangle &= -\pi^2 G_2. \end{aligned} \quad (2.3)$$

Here one always assumes that the product of the field strengths is normal ordered with respect to the “perturbative vacuum”. Thus (2.3) should be interpreted in the following sense: in the physical vacuum the chromomagnetic field fluctuates with bigger, the chromoelectric field with smaller amplitude than in the “perturbative vacuum”.

The extension of this condensate idea to a correlation function of gluon fields at different space-time points was considered in [14, 15, 2, 16, 17]. In this approach the vacuum is in essence characterized by two numbers: the strength of the vacuum fields, given by G_2 , and the correlation length a . This latter number is well determined phenomenologically [12, 18] to be

$$a \simeq 0.35 \text{ fm}. \quad (2.4)$$

A physical picture of the QCD vacuum state incorporating the gluon condensate G_2 and the finite correlation length a is the domain picture as discussed in [2]. In Euclidean space we can think of having domains in the vacuum of linear size $\simeq a$ (cf. Fig. 3 of [2]). Inside one domain the colour fields are highly correlated. From one domain to the next the correlation is small. Of course, the orientation of the colour fields inside a domain and the domain sizes fluctuate. If we translate this picture naively to Minkowski space, we arrive at colour correlations there being characterized by *invariant* distances of order a . Then the colour fields at the origin of Minkowski space, for instance, should be highly correlated with the fields in the region

$$|x^2| \lesssim a^2 \quad (2.5)$$

(cf. Fig. 1). Here it is important to remember that the gluon field strengths at point x are to be compared with the gluon field strengths at the origin after parallel transport on a straight line from x to 0 (cf. [17, 18]).

Let us introduce an observer in the “femtouniverse”, i.e. an observer watching with a microscope of resolution much better than 1 fm a hadron which moves very fast in positive 3-direction. The observer will see quarks and gluons in the hadron. Consider for example a fast quark passing through the origin of the coordinate system in Fig. 1 on a nearly light-like world line. The above picture of the QCD vacuum implies that this fast quark spends a long time (from the point of view of the observer) in a highly correlated colour field.

In the following we will only consider “light” hadrons having no “heavy” valence quarks c, b . Then the hadron’s

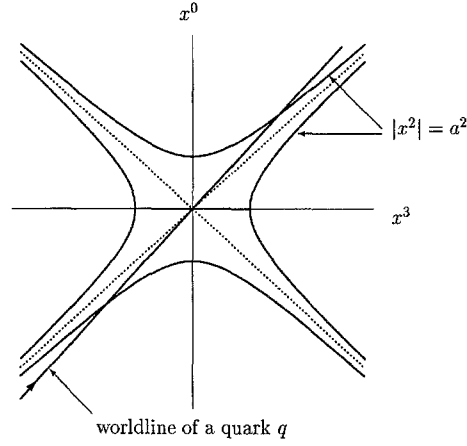


Fig. 1. Sketch of a “colour domain” in Minkowski space and of a quark from a fast hadron moving through it

radius $R \simeq 1 \text{ fm}$ is substantially larger than the correlation length a (2.4).

Let our observer now watch two quarks q_1, q_2 of the same hadron. We want to estimate the time interval over which q_1 , moving in one domain, can be considered as moving uncorrelated with q_2 .

Let E_h, E_1, E_2 be the energies of the hadron and of q_1, q_2 in a system where they all move fast in positive 3-direction and let m_q be the quark mass. For simplicity we consider the case where the transverse velocities of q_1 and q_2 are zero. The world lines of $q_{1,2}$ are then

$$y_i(t_i) \simeq \begin{pmatrix} t_i \\ \mathbf{y}_{iT} \\ y_i^3(0) + \left(1 - \frac{1}{2\gamma_i^2}\right) t_i \end{pmatrix}, \quad (i = 1, 2), \quad (2.6)$$

where

$$\gamma_i = (1 - \mathbf{v}_i^2)^{-1/2} = E_i/m_q \quad (2.7)$$

are the Lorentz γ factors for which we have assumed

$$\gamma_2 \geq \gamma_1 \gg 1. \quad (2.8)$$

We get now

$$\begin{aligned} (\Delta y)^2 &:= (y_1(t_1) - y_2(t_2))^2 \\ &\simeq -2(y_1^3(0) - y_2^3(0))(t_1 - t_2) - (\mathbf{y}_{1T} - \mathbf{y}_{2T})^2 \\ &\quad - (y_1^3(0) - y_2^3(0))^2 + \mathcal{O}\left(\frac{1}{\gamma_i^2}\right). \end{aligned} \quad (2.9)$$

Typically q_1 and q_2 will have a transverse separation of order R , i.e. substantially larger than the correlation length a :

$$|\mathbf{y}_{1T} - \mathbf{y}_{2T}| = \mathcal{O}(R). \quad (2.10)$$

The longitudinal separation of q_1 and q_2 on the other hand will be Lorentz-contracted and can be estimated to be of order R/γ_1 :

$$|y_1^3(0) - y_2^3(0)| \simeq R/\gamma_1. \quad (2.11)$$

Thus we obtain from (2.9)–(2.11), neglecting the terms of order $1/\gamma_i^2$:

$$(t_1 - t_2) \frac{R}{\gamma_1} c_1 \simeq c_2 R^2 + \Delta y^2 \quad (2.12)$$

where c_1, c_2 are constants with $|c_1|, |c_2|$ of order 1. If we require now

$$|(\Delta y)^2| \lesssim a^2 \ll R^2 \quad (2.13)$$

the solution of (2.12) is

$$t_1 - t_2 \simeq \frac{c_2}{c_1} \gamma_1 R + \frac{\gamma_1}{c_1 R} \Delta y^2. \quad (2.14)$$

Setting here for an order of magnitude estimate $c_1 = \pm 1$ and $c_2 = \pm 1$ we get:

$$|t_1 - t_2| \simeq \gamma_1 R \left(1 \pm \frac{a^2}{R^2} \right). \quad (2.15)$$

This means the following: The quark q_2 is in the same colour domain as q_1 at time t_1 only for the following intervals of the time t_2 :

$$t_1 - \gamma_1 R \left(1 + \frac{a^2}{R^2} \right) \lesssim t_2 \lesssim t_1 - \gamma_1 R \left(1 - \frac{a^2}{R^2} \right) \quad (2.16)$$

and

$$t_1 + \gamma_1 R \left(1 - \frac{a^2}{R^2} \right) \lesssim t_2 \lesssim t_1 + \gamma_1 R \left(1 + \frac{a^2}{R^2} \right). \quad (2.17)$$

Conversely, for time separations

$$|t_1 - t_2| \lesssim \gamma_1 R \left(1 - \frac{a^2}{R^2} \right) \simeq \gamma_1 R \quad (2.18)$$

q_1 and q_2 are in *uncorrelated* domains. Note that the time interval (2.18) is large if γ_1 is large.

Introducing the energy fraction $x_1 = E_1/E_h$ of hadron h carried by q_1 we can write (2.18) as

$$|t_1 - t_2| \lesssim \frac{E_h}{m_q} x_1 R =: \Delta t(x_1). \quad (2.19)$$

Our observer can interpret this result as follows. Two hard partons, $x_2 \geq x_1 = \mathcal{O}(1)$ are uncorrelated for a very long relative time separation $\Delta t(x_1)$. Short time correlations only occur if q_1 is a “wee” parton, i.e. a parton with energy less than some fixed energy $E_{\text{wee}}^{\text{max}} \simeq 0.5 \text{ GeV} \simeq a^{-1}$, say. This means for the energy fraction x_{wee} carried by a “wee” parton:

$$x_{\text{wee}} \leq E_{\text{wee}}^{\text{max}}/E_h \simeq \frac{0.5 \text{ GeV}}{E_h} \simeq \frac{1}{aE_h}. \quad (2.20)$$

We find then that for all “non-wee” quarks, i.e. for all quarks having $x_2 \geq x_1 > E_{\text{wee}}^{\text{max}}/E_h$ the difference of times over which they travel in an uncorrelated fashion satisfies

$$\Delta t(x_1) \gtrsim \frac{1}{m_q} E_{\text{wee}}^{\text{max}} R \simeq \frac{1}{m_q} \frac{R}{a} =: \Delta t_0. \quad (2.21)$$

We think it is reasonable to put here for m_q the current quark masses $m_u, m_d \simeq 5\text{--}10 \text{ MeV}$ [19], since we are

concerned with “non-wee” partons. Then

$$\Delta t_0 \simeq 50 \text{ fm}, \quad (2.22)$$

which is a very large time indeed for hadronic interactions.

Of course, in reality the quarks do not travel on parallel straight lines. In fact the effects which we discuss in this paper are due to the bending of the quark trajectories in the vacuum chromomagnetic fields. Thus the above exercise should only be taken as a rough estimate of how the vacuum structure with a *small* invariant correlation length a (2.4) can produce very *large* time and length scales $\Delta t(x_1) \gtrsim \Delta t_0$ (2.21), (2.22) for fast hadrons in Minkowski space. We will argue below that this allows us to add the contributions to synchrotron radiation from the partons in the hadrons incoherently.

At this point we can make a comment on the Drell-Yan process

$$h_1 + h_2 \rightarrow V + X, \quad (2.23)$$

where $h_{1,2}$ are the initial hadrons and V is the produced vector boson ($V = \gamma^*, W, Z$). In [20] possible nonperturbative effects related to the QCD vacuum structure were discussed for this reaction. The basic process leading to (2.23) is the annihilation of a quark q and an antiquark \bar{q} with the production of the vector boson V :

$$q + \bar{q} \rightarrow V. \quad (2.24)$$

Let the $q\bar{q}$ -annihilation occur at the origin of the coordinate system in Fig. 2 and let $q(\bar{q})$ be a parton of $h_1(h_2)$. It is clear that here q and \bar{q} have travelled for a time $t \gtrsim \Delta t_0$ (2.22) in a correlated colour background field. Thus there is ample time for a correlation of their spins to occur as suggested in [2, 20]. Indeed, if we estimate the build-up time τ_{pol} for the polarization due to gluon spin flip synchrotron radiation from the analogous formula from electrodynamics [21], we get for the quark q :

$$\tau_{\text{pol}} \simeq \frac{1}{\gamma_q^2} \frac{m_q^5}{\alpha_s (gB_c)^3}, \quad (2.25)$$

where gB_c is the effective chromomagnetic background field strength times the coupling constant and γ_q is the

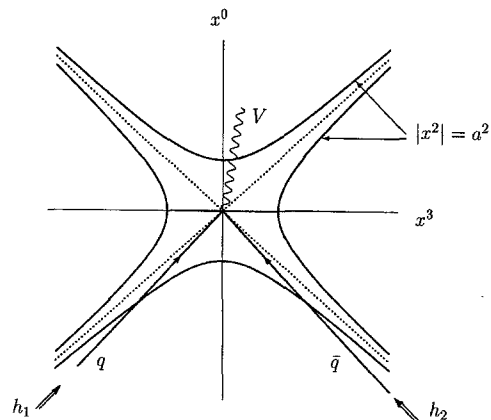


Fig. 2. Annihilation of a $q\bar{q}$ pair and production of a vector boson $V = \gamma^*, Z, W$ in a colour domain. Here q and \bar{q} come from two different hadrons h_1 and h_2 , respectively

Lorentz factor for the quark. For the antiquark a similar formula holds. Then certainly $\Delta t_0 \gg \tau_{\text{pol}}$ for large $\gamma_q, \gamma_{\bar{q}}$. Of course, the estimate (2.25) for τ_{pol} applies to a static B field and taking it over for the vacuum “background” fields is highly debatable. However, what we may conclude from (2.25) is that for $m_q \rightarrow 0$ the quark’s spin motion and corresponding spin-flip synchrotron radiation are infrared sensitive effects related to the vacuum gluon fields. Thus even if we are unable at present to calculate τ_{pol} there is no reason for it to be infinite as one would expect for the perturbative vacuum where $gB_c = 0$.

We return now to photon “synchrotron” radiation in a hadronic collision. For definiteness we consider a nucleon-nucleon collision with the production of n hadrons

$$N_1(p_1) + N_2(p_2) \rightarrow h_1(p'_1) + \dots + h_n(p'_n) \quad (2.26)$$

in the overall c.m. system.

In [2] we have estimated the number of synchrotron photons emitted from the nucleons in the initial state. Let \mathbf{k}, ω be the photon momentum and energy in the overall c.m. system. Then we obtain from (5.21), (5.22) of [2] for the photons from $N_1(p_1)$ in (2.26):

$$\omega \frac{d^3 n_\gamma^{(N_1)}}{d^3 k} = \frac{\alpha}{\omega^{4/3}} (l_{\text{eff}})^{2/3} S^{(N_1)}(\hat{\mathbf{p}}_1 \cdot \hat{\mathbf{k}}) \quad (2.27)$$

where $\hat{\mathbf{p}}_1 = \mathbf{p}_1/|\mathbf{p}_1|$, $\hat{\mathbf{k}} = \mathbf{k}/|\mathbf{k}|$ and

$$l_{\text{eff}} = \frac{\sigma}{gB_c}, \quad (2.28)$$

$$\begin{aligned} S^{(N_1)}(\hat{\mathbf{p}}_1 \cdot \hat{\mathbf{k}}) &= \frac{1}{2\pi^2} \frac{\Gamma^2(\frac{2}{3}) 6^{1/3}}{2 \ln(P/P_0)} \\ &\times \int_{-\chi_0}^{\chi_0} d\chi \Theta(\cos \vartheta^* + \tanh \chi) (\cosh \chi)^{-2/3} \\ &\times (1 + \cos \vartheta^* \tanh \chi)^{-4/3} \left(\frac{\cos \vartheta^* + \tanh \chi}{\sin \vartheta^*} \right)^{2/3} \\ &\times \int_0^{\psi_m(\chi)} d\psi \psi^{-1/3} F_2^{N_1} \left(\frac{\psi}{\psi_m(\chi)} \right) e^{-\psi^{2/2}}, \end{aligned} \quad (2.29)$$

$$\cos \vartheta^* = \hat{\mathbf{p}}_1 \cdot \hat{\mathbf{k}}, \quad (0 \leq \vartheta^* \leq \pi), \quad (2.30)$$

$$\psi_m(\chi) = \frac{P \sin \vartheta^*}{\sigma |\cos \vartheta^* + \tanh \chi| \cosh \chi} e^\chi, \quad (2.31)$$

$$P = p_1^0 \simeq \frac{\sqrt{s}}{2}, \quad \chi_0 = \ln(P/P_0). \quad (2.32)$$

As explained in [2], we obtained these formulae by using the synchrotron emission formulae for a constant chromomagnetic field in a particular reference frame and then averaging incoherently over all reference frames where both nucleons N_1 and N_2 move fast such that we can use the parton picture for them. In this way we introduced a cutoff parameter P_0 , the minimal nucleon momentum for the parton picture to be applicable. We set $P_0 = 1.5$ GeV here. The quantity σ is the mean transverse momentum of the quarks in the hadrons. We set

$$\sigma = 300 \text{ MeV} \quad (2.33)$$

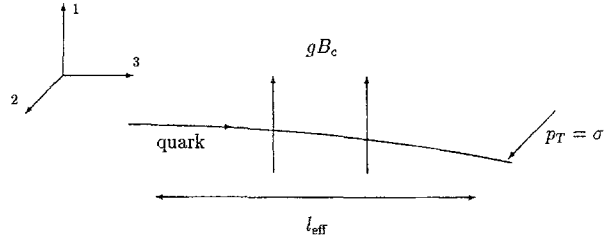


Fig. 3. A quark moving in 3-direction in a transverse (in 1-direction) chromomagnetic field of strength gB_c and picking up a transverse momentum (in 2-direction) of magnitude σ over a length l_{eff} . Here σ is the mean transverse momentum of quarks in the hadron

and we think that this number should be correct to ± 100 MeV. The quantity gB_c is, as in (2.25), the effective chromomagnetic background field strength times the coupling constant. Finally, l_{eff} (2.28) is the length or time a fast quark has to travel in a transverse background field of strength gB_c in order to pick up a transverse momentum of magnitude σ (cf. Fig. 3). $F_2^{N_1}$ is the usual structure function of the nucleon known from deep inelastic electron and muon nucleon scattering.

From the nucleon N_2 in the initial state of the reaction (2.26) we get of course a similar contribution of synchrotron photons:

$$\omega \frac{d^3 n_\gamma^{(N_2)}}{d^3 k} = \frac{\alpha}{\omega^{4/3}} (l_{\text{eff}})^{2/3} S^{(N_2)}(\hat{\mathbf{p}}_2 \cdot \hat{\mathbf{k}}), \quad (2.34)$$

where $S^{(N_2)}$ is obtained from (2.29) with obvious replacements: $F_2^{N_1} \rightarrow F_2^{N_2}$, $\vartheta^* \rightarrow \vartheta^*(\mathbf{k}, \mathbf{p}_2)$.

In the discussion above we have added the contributions of synchrotron photons from the partons in each nucleon N_1, N_2 incoherently and we have done the same for the total contributions from N_1 and N_2 . This needs some justification.

As we have seen in chapter 2, two partons of the same hadron travel for most of the time in different colour domains, i.e. the gluonic field strengths at their world lines are for most of the time uncorrelated. This means that their wiggling in the colour background fields is mostly uncorrelated. Thus interference terms from the emission of synchrotron photons by two partons will tend to average to zero. This is elaborated on in Appendix A.

To add the contributions from N_1 and N_2 incoherently seems quite a harmless assumption to us, since for any given background chromomagnetic field the photons from the partons of N_1 and N_2 will populate widely different regions of phase space.

We will now argue that from the final state hadrons in (2.26) we will also get synchrotron photons. In the hadronic collision quarks, antiquarks, and gluons from the original hadrons will be deflected, and new partons will be created as well. These final state partons will recombine to form hadrons. We can for instance think of the mechanisms discussed in the LUND model for particle production (for a review cf. [22]). Shortly after the collision, however, these hadrons did not yet have time to “dress” themselves with soft synchrotron photons, a process which will, as we shall see, take a time of order 20 fm. Thus initially we get “undressed” hadrons $h^{(0)}$. A state for

a physical hadron h can be expanded schematically as follows:

$$|h\rangle \simeq |h^{(0)}\rangle + e|h^{(0)}\gamma\rangle, \quad (2.35)$$

where the amplitude for $|h^{(0)}\gamma\rangle$ is due to our synchrotron effect and gives the photon emission if h is in the initial state. Reversing this we get

$$|h^{(0)}\rangle \simeq |h\rangle - e|h\gamma\rangle, \quad (2.36)$$

which we interpret as follows: The originally produced “naked” hadron $h^{(0)}$ will lead with amplitude $\simeq 1$ to a physical final state hadron h but also with some amplitude of order e to the emission of a “synchrotron” photon in addition. We discuss the meaning of (2.35) and (2.36) on a more formal level in Appendix B. The amplitudes for the photon emission in (2.35) and (2.36) differ only by the overall sign. Thus we should get a contribution to synchrotron photons from each final state hadron h with a spectrum given again by (2.27) with suitable replacements:

$$\omega \frac{d^3 n_\gamma^{(h)}}{d^3 k} = \frac{\alpha}{\omega^{4/3}} (l_{\text{eff}})^{2/3} S^{(h)}(\hat{\mathbf{p}}_h \cdot \hat{\mathbf{k}}). \quad (2.37)$$

Here $S^{(h)}$ is as in (2.29) with the replacements $F_2^{N_1} \rightarrow F_2^h$, $\mathcal{G}^* \rightarrow \mathcal{G}(\mathbf{k}, \mathbf{p}_h)$.

We can now put everything together. For inelastic collisions

$$p(p_1) + N(p_2) \rightarrow \text{hadrons } h \quad (2.38)$$

we predict the number of synchrotron photons per inelastic collision in the overall c.m. system as

$$\omega \frac{d^3 n_\gamma^{(\text{syn})}}{d^3 k} = \frac{\alpha}{\omega^{4/3}} (l_{\text{eff}})^{2/3} \Sigma(\hat{\mathbf{p}}_1 \cdot \hat{\mathbf{k}}), \quad (2.39)$$

where

$$\begin{aligned} \Sigma(\hat{\mathbf{p}}_1 \cdot \hat{\mathbf{k}}) &= S^{(N_1)}(\hat{\mathbf{p}}_1 \cdot \hat{\mathbf{k}}) + S^{(N_2)}(-\hat{\mathbf{p}}_1 \cdot \hat{\mathbf{k}}) \\ &+ \sum_h \frac{1}{\sigma_{\text{inel}}(N_1 N_2)} \int \frac{d^3 p_h}{E_h} \\ &\times \left(E_h \frac{d^3 \sigma}{d^3 p_h}(N_1 N_2 \rightarrow hX) \right) \cdot S^{(h)}(\hat{\mathbf{p}}_h \cdot \hat{\mathbf{k}}). \end{aligned} \quad (2.40)$$

Here h runs over all produced hadron species. We have in (2.40) added the contributions of all hadrons from the initial and final state incoherently. We think that this is justified since the time scale of the hadronic collision is of the order of 2–3 fm and thus very short compared to the emission or “dressing” time of order 20 fm involved in our synchrotron effect. Thus we treat the collision in a sort of “sudden approximation” well known in quantum mechanics (cf. e.g. [23]).

The photon spectrum from hadronic bremsstrahlung was calculated for multiparticle production in hadron-hadron collisions in [24] on the basis of Low’s theorem [1]. One finds for emission angles of the photon not too close to the collision axis:

$$\omega \frac{d^3 n_\gamma^{(\text{br})}}{d^3 k} \propto \frac{1}{\omega^2 [1 - (\hat{\mathbf{p}}_1 \cdot \hat{\mathbf{k}})^2]}. \quad (2.41)$$

From (2.39) and (2.41) we get for the ratio of synchrotron to bremsstrahlung photons:

$$\frac{\omega d^3 n_\gamma^{(\text{syn})}}{d^3 k} \bigg/ \frac{\omega d^3 n_\gamma^{(\text{br})}}{d^3 k} \propto \omega^{2/3}. \quad (2.42)$$

Thus our synchrotron effect vanishes relative to bremsstrahlung for $\omega \rightarrow 0$ and Low’s theorem is respected. For very small ω the synchrotron effect vanishes relative to bremsstrahlung faster than $\omega^{2/3}$ (2.42) since there the incoherent summation of the contributions of the different partons is no longer justified. In Appendix A, below, we estimate that this incoherence assumption should break down for

$$|\mathbf{k}_T| \lesssim 3.5 \text{ MeV}, \quad (2.43)$$

where $|\mathbf{k}_T| = |\omega \sin \mathcal{G}^*|$.

3 Comparison with experiment

There are a number of experiments on prompt photon production in high energy hadron-hadron collisions. The earliest experiment [25] found a γ -signal compatible with bremsstrahlung from the hadrons. Subsequent experiments [26–29] reported numbers of soft photons partly in great excess over the expectations from hadronic bremsstrahlung. On the other hand the authors of the experiment [3] give only upper limits on the possible presence of “anomalous” soft photons and conclude that there cannot be too many of them. An anomalous yield of prompt photons was also seen in muon-proton deep inelastic scattering [30]. Here and in the following we will use the words “anomalous yield of photons” or simply “anomalous photons” for a yield exceeding the theoretical expectation from bremsstrahlung.

On the theoretical side in [2] a prediction for the existence of anomalous soft photons in hadron-hadron and lepton-hadron scattering as well as jet production in e^+e^- -annihilation was made. This was *before* the publication of the results of the first experiment [26] which saw anomalously large numbers of soft photons. Subsequently two other theoretical models for the production of anomalous soft photons were proposed. The “soft annihilation model” [31, 32] which had previously been used to describe soft lepton pair production [33, 34] and the “glob” model [35, 36]. We will comment on how to distinguish these models below.

In this section we will first compare our theoretical expressions (2.39), (2.40) to the experimental data from [3] and then make some comments concerning the data from [26–29]. In the experiment [3] soft photons produced in p -Be collisions at 450 GeV incident proton momentum were measured. We have thus the collision

$$p(p_1) + N(p_2) \rightarrow \text{hadrons} + \gamma(k) \quad (3.1)$$

where N stands for the average nucleon in the Be nucleus. The c.m. energy of the pN collision is

$$\sqrt{s} = 29.09 \text{ GeV}. \quad (3.2)$$

The final hadronic state contains in most of the cases two nucleons plus pions. We will neglect other particle compositions of the final state in the following.

In Fig. 4 we reproduce Fig. 5 of [3] with the normalization provided to us by H.J. Specht. Here we use the variables in the overall c.m. system:

$$\begin{aligned} k_T &= (\mathbf{k}^2 - (\hat{\mathbf{p}}_1 \cdot \mathbf{k})^2)^{1/2}, \\ y &= -\ln \tan(\mathcal{G}^*/2), \\ \mathcal{G}^* &= \angle(\mathbf{k}, \hat{\mathbf{p}}_1). \end{aligned} \quad (3.3)$$

Expressed in these variables our prediction for synchrotron photons (2.39), (2.40) reads

$$\frac{d^2 n_\gamma^{(\text{syn})}}{dk_T dy} = \frac{2\pi\alpha(l_{\text{eff}})^{2/3}}{k_T^{1/3}} (\sin \mathcal{G}^*)^{4/3} \Sigma(\cos \mathcal{G}^*). \quad (3.4)$$

In the sum over the final state hadrons h in (2.40) we include 2 nucleons plus pions, as mentioned above. Consider first the two nucleons. These are “leading” particles and carry away a substantial fraction of the available energy in forward and backward direction, respectively (cf. [37]). We estimate their contribution to Σ to be approximately the same as for the initial state nucleons. Next we consider the contribution to Σ from π^+ , π^- , π^0 . Due to isospin and charge conjugation invariance the structure functions F_2 for π^+ , π^- and π^0 are equal. At least approximately also the inclusive cross sections for π^+ , π^- and π^0 are equal [37]. Making this assumption, we obtain from (2.40) for the reaction (3.1)

$$\begin{aligned} \Sigma(\cos \mathcal{G}^*) &= 2S^{(p)}(\hat{\mathbf{p}}_1 \cdot \hat{\mathbf{k}}) + 2S^{(N)}(-\hat{\mathbf{p}}_1 \cdot \hat{\mathbf{k}}) \\ &+ 3 \frac{1}{\sigma_{\text{inel}}(pN)} \int \frac{d^3 p_\pi}{E_\pi} \left(E_\pi \frac{d^3 \sigma}{d^3 p_\pi} (pN \rightarrow \pi X) \right) S^{(\pi)}(\hat{\mathbf{p}}_\pi \cdot \hat{\mathbf{k}}). \end{aligned} \quad (3.5)$$

To calculate Σ numerically we used the following input. For the structure functions F_2^p, F_2^N entering in $S^{(p)}, S^{(N)}$ (cf. (2.29)) we used the set D'_0 from the MRS analysis [38] with the Q^2 value taken to be 4 GeV^2 . In (6.37) of [39] we have estimated the “equivalent” Q^2 value of deep inelastic lepton-hadron scattering for a hadronic collision of c.m. energy \sqrt{s} to be

$$Q^2 \simeq \sqrt{s} \cdot 0.05 \text{ GeV}. \quad (3.6)$$

For $\sqrt{s} \simeq 30 \text{ GeV}$ this gives $Q^2 = 1.5 \text{ GeV}^2$. We prefer to use a slightly higher Q^2 value since structure functions at $Q^2 = 1.5 \text{ GeV}^2$ are more likely to be contaminated by higher twist effects and thus their interpretation in terms of parton densities is more questionable. We use the set D'_0 which has structure functions $F_2(x)$ with a *finite* value at $x = 0$. This we consider reasonable for application in a hadronic reaction. We may cite here the duality arguments between parton and produced hadron distributions put forward already in the pioneering work of Feynman [40]: The rapidity distribution of the pions produced in a nucleon-nucleon collision is flat at zero c.m. rapidity. Assuming the same to hold for the partons in the nucleons from which the pions originate leads to a behaviour

$$F_2^N(x) \rightarrow \text{const.} \quad \text{for } x \rightarrow 0. \quad (3.7)$$

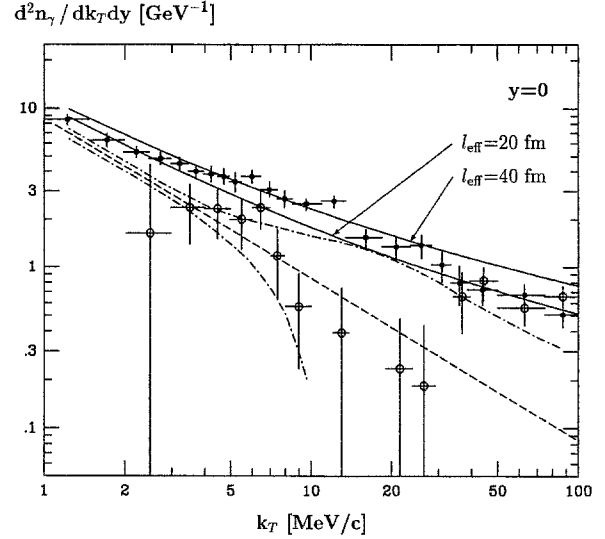


Fig. 4. The $|k_T|$ distribution for direct photons emitted at c.m. rapidity $y = 0$ in p -Be collisions at 450 GeV incident proton momentum from [3]. The normalization is according to a private communication by H.J. Specht. The background of decay photons is subtracted. The dashed line gives the expected yield of photons from hadronic bremsstrahlung, the dash-dotted lines show the upper and lower limits including the systematic errors in the shape of the decay background and the bremsstrahlung calculation (cf. [3]). The lower (upper) solid line is the result of our calculation for synchrotron photons ((3.4) ff.) with $l_{\text{eff}} = 20 \text{ fm}$ ($l_{\text{eff}} = 40 \text{ fm}$) added to the spectrum of hadronic bremsstrahlung

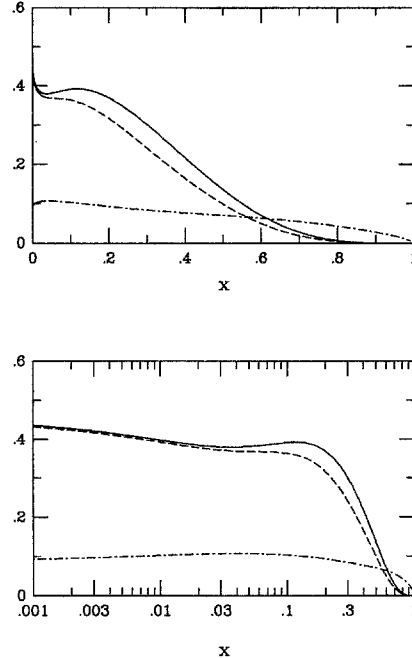


Fig. 5. The structure functions $F_2^p(x)$, $F_2^N(x)$ (N = average of proton and neutron) and $F_2^{\pi}(x)$ for $Q^2 = 4 \text{ GeV}^2$ used in this paper. F_2^p , F_2^N are from set D'_0 of [38], F_2^{π} is from [43]. $F_2^p(x)$ —; $F_2^N(x)$ ---; $F_2^{\pi}(x)$ - - - - -

On the other hand, a significant rise of $F_2^p(x, Q^2)$ for $x \lesssim 5 \cdot 10^{-3}$ and $Q^2 \gtrsim 9 \text{ GeV}^2$ has been observed at HERA [41]. This can hardly be relevant for our case since for a nucleon energy in the c.m. system $E_N = 15 \text{ GeV}$, values

of $x \leq 5 \cdot 10^{-3}$ correspond to parton momenta $E_{\text{parton}} \leq 45$ MeV. This is well in the “wee” region where we certainly should not use parton distributions fitting high Q^2 data and evolving the structure functions obtained in this way to $Q^2 \simeq 4 \text{ GeV}^2$ using the leading twist theory only. Of course, for very high energy hadron-hadron collisions the situation will be different. But this is beyond the scope of the present work. We also note that a recent fixed target muon-nucleon scattering experiment [42] presented preliminary results for structure functions at low x and low Q^2 supporting rather the D'_0 type parton distributions over the singular D'_- type of [38].

The structure function F_2^p was taken from [43]. We use here again $Q^2 = 4 \text{ GeV}^2$. Our structure function input is shown in Fig. 5.

For the inelastic pN cross section we take

$$\sigma_{\text{inel}}(pN) = 33.2 \text{ mb}, \quad (3.8)$$

where we assumed $\sigma_{\text{inel}}(pp) = \sigma_{\text{inel}}(pn)$ and took $\sigma_{\text{inel}}(pp)$ for $\sqrt{s} = 29 \text{ GeV}$ from the fit on page III.77 of [44]. For the mean pion multiplicity at $\sqrt{s} = 29 \text{ GeV}$ we took

$$\frac{1}{3}(n_{\pi^+} + n_{\pi^-} + n_{\pi^0}) = 3.74 \quad (3.9)$$

as deduced from the fits given in [45]. For the pion inclusive distribution we used the parametrization given in [46], but rescaled to give, when integrated, the pion multiplicity (3.9):

$$E \frac{d^3\sigma}{d^3p_\pi}(pN \rightarrow \pi X) = \frac{AB^C}{(E_T + B)^C} f(y_\pi, p_T) \times \begin{cases} e^{-p_T} & \text{for } p_T < 1 \\ e^{-D(p_T - 1)/\sqrt{s} - 1} & \text{for } p_T > 1 \end{cases} \quad (p_T \text{ in GeV}), \quad (3.10)$$

where

$$E_T = \sqrt{p_T^2 + m_\pi^2},$$

$$y_\pi = \frac{1}{2} \ln \frac{E + p_\parallel}{E - p_\parallel},$$

$$E_{\text{max}} = \frac{1}{2\sqrt{s}}(s + m_\pi^2 - 4m_p^2),$$

$$p_{\text{max}} = \sqrt{E_{\text{max}}^2 - m_\pi^2},$$

$$p_{\parallel\text{max}} = \sqrt{p_{\text{max}}^2 - p_T^2},$$

$$y_{\text{max}}(p_T) = \ln \frac{E_{\text{max}} + p_{\parallel\text{max}}}{E_T},$$

$$f(y_\pi, p_T) = \exp \left[-\frac{\alpha}{(y_{\text{max}}(p_T) - |y_\pi|)^\beta} \right],$$

$$A = \frac{3.74}{2.89} \cdot 3.78 \cdot 10^{-24} \text{ cm}^2 \text{ GeV}^{-2},$$

$$B = 2 \text{ GeV},$$

$$C = 12.3,$$

$$D = 23 \text{ GeV},$$

$$\alpha = 5.13,$$

$$\beta = 0.38. \quad (3.11)$$

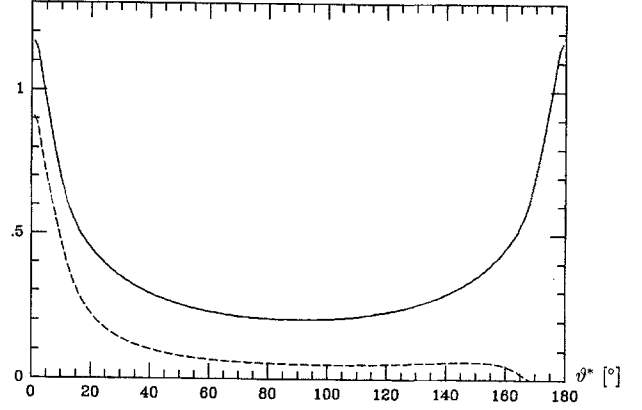


Fig. 6. The quantities $2S^{(p)}(\cos \vartheta^*)$ (---) and $\Sigma(\cos \vartheta^*)$ (—) (cf. (3.5)) related to the angular distribution of synchrotron photons in the overall c.m. frame according to (3.4). Here ϑ^* is the emission angle of the photon: $\cos \vartheta^* = \hat{\mathbf{p}}_1 \cdot \hat{\mathbf{k}}$

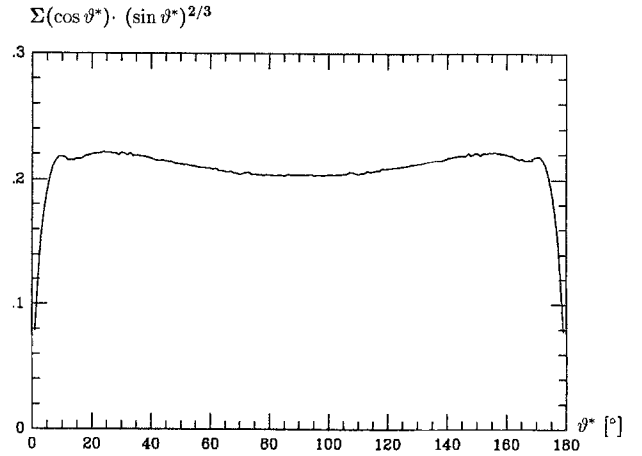


Fig. 7. The quantity $(\sin \vartheta^*)^{2/3} \cdot \Sigma(\cos \vartheta^*)$ as function of ϑ^* . Over a large range of ϑ^* this quantity is nearly constant

Using these inputs we can calculate $S^{(p)}$, $S^{(N)}$ and Σ . For the parameters P/σ and P/P_0 occurring in the integral (2.29) we took

$$P/\sigma = 50, \quad P/P_0 = 10 \quad (3.12)$$

for the p and N case and

$$P/\sigma = P/P_0 = 10 \quad (3.13)$$

for the pion case. We found that the results for photon emission angles $20^\circ \leq \vartheta^* \leq 160^\circ$ were insensitive to variations in these parameters over a reasonable range. In Fig. 6 we show $2S^{(p)}(\cos \vartheta^*)$ and $\Sigma(\cos \vartheta^*)$ as function of ϑ^* . As already noted in [2], we expect that $\Sigma(\cos \vartheta^*) \propto (\sin \vartheta^*)^{-2/3}$ for most ϑ^* with the exception of angles very close to $\vartheta^* = 0^\circ$ and $\vartheta^* = 180^\circ$. This is confirmed by the numerical calculations as shown in Fig. 7.

Having determined Σ , our synchrotron radiation formula (3.4) contains as unknown parameter only l_{eff} . We did not try to make a “best fit” for l_{eff} from the data of Fig. 4. Instead we looked at the result for the prompt photon spectrum adding to the hadronic bremsstrahlung as given in [3] the synchrotron photons (3.4) with various

values of l_{eff} . We found that the data is quite consistent with l_{eff} in the following range

$$20 \text{ fm} \lesssim l_{\text{eff}} \lesssim 40 \text{ fm}. \quad (3.14)$$

In Fig. 4 we show our results for $l_{\text{eff}} = 20 \text{ fm}$ and $l_{\text{eff}} = 40 \text{ fm}$ superimposed on the data.

We should be careful with the interpretation of our results. The authors of [3] do *not* claim that there is an excess over the hadronic bremsstrahlung in the photon spectrum. They interpret their data as giving upper limits on the presence of additional sources of direct photons at small transverse momentum. So what we can conclude from our calculation is that the data is consistent with the presence of “synchrotron photons” as additional source with $l_{\text{eff}} \lesssim 40 \text{ fm}$. Taking the error bars of the data in Fig. 4 seriously we may even conclude that the data prefer bremsstrahlung plus synchrotron photons over bremsstrahlung photons only. It would clearly be very interesting to have more precise data which would allow to draw more definite conclusions.

At this point we should discuss the data on soft photon production in hadron-hadron collisions from [26–29]. These experiments see a large excess of soft photons over the bremsstrahlung level. For us theorists the experimental situation – all data together – is too confusing, so we will not attempt to fit everything. Furthermore, comparison of theory with some published experimental results would require information on experimental cuts, detector efficiencies etc. which is not available to us. Anyway, our prediction of synchrotron photons is given in (2.39), (2.40) and this should be for experimentalists a target to shoot down.

When most of the present paper was written we received a preprint [47] where the soft annihilation model and the glob model are compared with data. Here we would like to point out that the dependence of the number $n_{\gamma}^{(\text{an})}$ of anomalous soft photons per event on the hadronic multiplicity n_h provides a way to distinguish between these models and our synchrotron effect. According to [47] the soft annihilation model gives $n_{\gamma}^{(\text{an})} \propto (n_h)^2$, in the glob model $n_{\gamma}^{(\text{an})}$ is independent of n_h . For our synchrotron effect the multiplicity dependence of $n_{\gamma}^{(\text{syn})}$ can be read off from (2.39), (2.40). In essence we have

$$n_{\gamma}^{(\text{syn})} = \int \frac{d^3 k}{\omega} \left(\omega \frac{d^3 n_{\gamma}^{(\text{syn})}}{d^3 k} \right) \propto n_h + 2, \quad (3.15)$$

where the 2 comes from the contribution of the initial state hadrons.

4 Synchrotron radiation and electromagnetic formfactors of hadrons

We have argued in Sect. 2 that the colour fields in the vacuum should give a contribution to the virtual photon cloud of hadrons and we made an estimate of the distribution of these photons using the synchrotron radiation formulae. Consider now any reaction where a quasi-real photon is emitted from a hadron with the hadron staying intact and the photon interacting subsequently. In

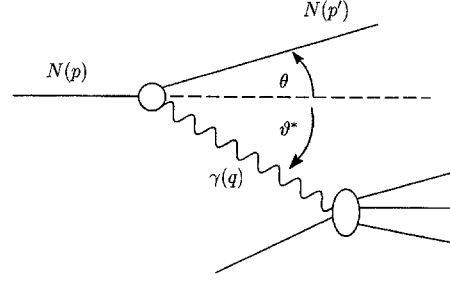


Fig. 8. A nucleon interacting by emission of a quasi-real photon

Fig. 8 we draw the corresponding diagram for a nucleon N :

$$N(p) \rightarrow N(p') + \gamma(q). \quad (4.1)$$

The flux of these quasi-real photons is well known. The first calculations in this context are due to Fermi, Weizsäcker, and Williams [48]. For us the relevant formula is given in (D.4) of [49]. Let E be the energy of the initial nucleon, $G_E^N(Q^2)$ its electric Sachs formfactor, and let ω and $q^2 = -Q^2$ be the energy and mass of the virtual photon. Then the distribution of quasi-real photons in the fast moving nucleon is given by

$$dn_{\gamma}^{(\text{excl})} = \frac{\alpha}{\pi} \frac{d\omega}{\omega} \frac{dQ^2}{Q^2} [G_E^N(Q^2)]^2 \quad (4.2)$$

where we neglect terms of order ω/E and Q^2/m_N^2 and assume

$$Q^2 \gg Q_{\min}^2 \simeq \frac{m_N^2 \omega^2}{E^2}. \quad (4.3)$$

We call (4.2) the exclusive flux since the nucleon stays intact. Now we want to translate (4.2) into a distribution in ω and the angle ϑ^* of emission of the γ (cf. Fig. 8). We have from transverse momentum balance:

$$|\mathbf{q}| \sin \vartheta^* = |\mathbf{p}'| \sin \theta, \quad (4.4)$$

$$|\mathbf{q}|^2 \sin^2 \vartheta^* = |\mathbf{p}'|^2 (1 - \cos \theta)(1 + \cos \theta).$$

Furthermore we have:

$$Q^2 = 2(E E' - m_N^2 - |\mathbf{p}| |\mathbf{p}'| \cos \theta), \quad (4.5)$$

where $E = p^0$, $E' = p'^0 = E - \omega$. From this we get

$$\sin^2 \vartheta^* = \frac{1}{\omega^2 + Q^2} \frac{1}{|\mathbf{p}|^2} \left(\frac{1}{2} Q^2 - m_N^2 \frac{\omega^2}{E E' + |\mathbf{p}| |\mathbf{p}'| - m_N^2} \right) \times (E E' + |\mathbf{p}| |\mathbf{p}'| - m_N^2 - \frac{1}{2} Q^2). \quad (4.6)$$

For

$$E, E' \gg m_N, \omega \quad \text{and} \quad \omega^2 \gg Q^2 \quad (4.7)$$

this reduces to

$$\sin^2 \vartheta^* \simeq \frac{Q^2}{\omega^2}. \quad (4.8)$$

Inserting this in (4.2) gives

$$dn_{\gamma}^{(\text{excl})} \simeq \frac{2\alpha}{\pi} \frac{d\omega}{\omega} \frac{d\vartheta^*}{\sin \vartheta^*} [G_E^N(\omega^2 \sin^2 \vartheta^*)]^2. \quad (4.9)$$

The range in ϑ^* for which (4.9) is valid is obtained from (4.3) and (4.7), (4.8) as

$$\left(\frac{m_N}{E}\right)^2 \ll \sin^2 \vartheta^* \ll 1. \quad (4.10)$$

We will now make an “exclusive-inclusive connection” argument. In (2.27) we have calculated the total spectrum of synchrotron photons from a nucleon in an *inelastic* collision:

$$dn_{\gamma}^{(\text{incl})} = 2\pi\alpha \frac{d\omega}{\omega} d\vartheta^* \sin \vartheta^* \omega^{2/3} (l_{\text{eff}})^{2/3} S^{(N)}(\cos \vartheta^*). \quad (4.11)$$

We call this now the inclusive spectrum, since it can be thought of as the integral result of the synchrotron effect from the diagram of Fig. 8 and the corresponding ones, where instead of the outgoing nucleon $N(p')$ we allow an arbitrary hadronic state X to occur:

$$N(p) \rightarrow X(p') + \gamma(q). \quad (4.12)$$

The exclusive channel (4.1) is part of the inclusive sum and we will now require that it contains also a “synchrotron” piece, leading to the same power of ω as in (4.11). We can achieve this by requiring a term in the formfactor $G_E^N(Q^2)$ being proportional to $(Q^2)^{1/6}$. Then, indeed, we find from (4.9):

$$dn_{\gamma}^{(\text{excl})} \propto \frac{2\alpha}{\pi} \frac{d\omega}{\omega} d\vartheta^* \sin \vartheta^* \omega^{2/3} (\sin \vartheta^*)^{-4/3}. \quad (4.13)$$

The exclusive distribution (4.13) drops faster in angle than the inclusive one (4.11), where for ϑ^* satisfying (4.10) $S^{(N)}(\cos \vartheta^*) \propto (\sin \vartheta^*)^{-2/3}$. This is quite reasonable physically.

Thus we arrive at the following conclusion: The proton formfactor G_E^p should contain in addition to a “normal” piece connected with the total charge and the hadronic bremsstrahlung in inelastic collisions a piece $\propto (Q^2)^{1/6}$ connected with “synchrotron” radiation from the QCD vacuum. In our exclusive-inclusive connection argument we have neglected any interference between these two pieces since this can be expected to be very small in an inclusive sum. For the neutron which has total charge zero we would expect the “normal” piece in G_E^n to be quite small and the “anomalous” piece to be quite important for not too large Q^2 . Thus the neutron electric formfactor should be an interesting quantity to look for “anomalous” effects $\propto (Q^2)^{1/6}$.

In Fig. 9 we show the data on the electric formfactor of the neutron from [50, 51]. We superimpose the curve

$$G_{(\text{syn})}^n(Q^2) = 3.6 \cdot 10^{-2} \left(\frac{Q^2}{5 \text{ fm}^{-2}} \right)^{1/6} \quad (4.14)$$

which is normalized to the data at $Q^2 = 5 \text{ fm}^{-2}$. We see that except in the very low Q^2 region we get a decent description of the data. For $Q^2 \rightarrow 0$ (4.14) has to break down since $G_E^n(Q^2)$ is regular at $Q^2 = 0$. Indeed one knows the slope of $G_E^n(Q^2)$ for $Q^2 = 0$ from the scattering of

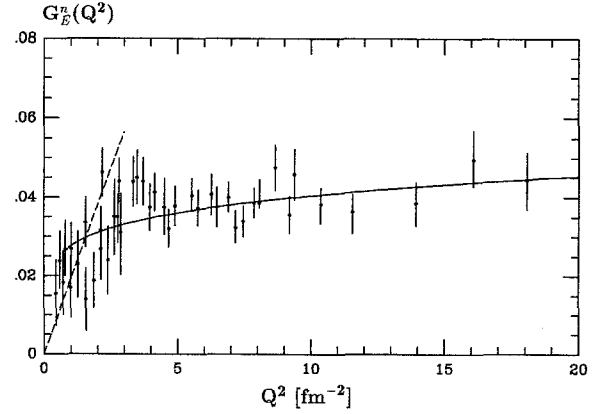


Fig. 9. The data for the electric formfactor of the neutron, $G_E^n(Q^2)$ from [50, 51]. Full line: our “synchrotron” prediction $\propto (Q^2)^{1/6}$ normalized to the data at $Q^2 = 5 \text{ fm}^{-2}$. Dashed line: the slope of $G_E^n(Q^2)$ at $Q^2 = 0$ as deduced from thermal neutron-electron scattering [52]

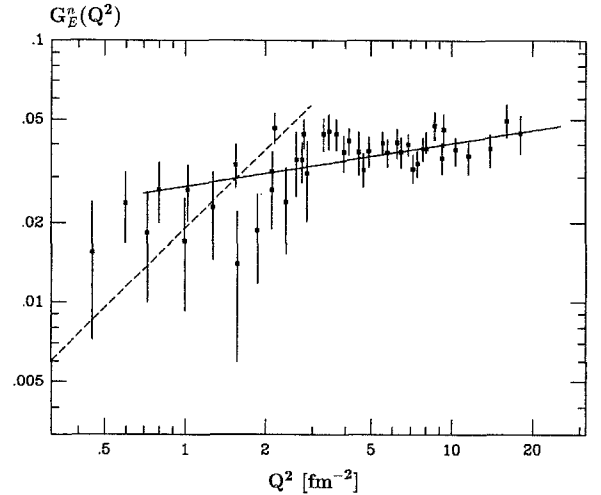


Fig. 10. Same as Fig. 9 but in a double logarithmic plot

thermal neutrons on electrons ([52] and references cited therein):

$$\left. \frac{dG_E^n(Q^2)}{dQ^2} \right|_{Q^2=0} = 0.019 \text{ fm}^2. \quad (4.15)$$

We see from Fig. 9 that the behaviour of $G_E^n(Q^2)$ has to change rather quickly as we go away from $Q^2 = 0$. In Fig. 10 we plot the formfactor in a double logarithmic diagram. A behaviour proportional to $(Q^2)^{1/6}$ would lead to a straight line with slope 1/6. We see again that within the errors this is consistent with the data in the range

$$0.5 \text{ fm}^{-2} \leq Q^2 \leq 20 \text{ fm}^{-2}. \quad (4.16)$$

Note that the square of the inverse correlation length a (2.4) gives

$$a^{-2} = (0.35 \text{ fm})^{-2} = 8.16 \text{ fm}^{-2}. \quad (4.17)$$

Thus it should not be surprising if we see effects of the QCD vacuum structure in the Q^2 range (4.16). Translating the findings (4.14), (4.16) into coordinate space we see that

according to our results the charge density $\rho(r)$ and the electromagnetic potential $V(r)$ of the neutron should behave as

$$\begin{aligned}\rho(r) &\propto r^{-10/3}, \\ V(r) &\propto r^{-4/3}\end{aligned}\quad (4.18)$$

in the following range for the radius r :

$$1.5 \text{ fm} \gtrsim r \gtrsim 0.2 \text{ fm}. \quad (4.19)$$

What about the electric formfactor of the proton, $G_E^p(Q^2)$? A piece proportional to $(Q^2)^{1/6}$ in $G_E^p(Q^2)$ should produce a rapid variation with Q^2 when going from $Q^2 = 0$ to $Q^2 \simeq 2 \text{ fm}^{-2}$ (cf. Fig. 9). This should be difficult to fit with the usual dipole formula:

$$G_{\text{Dipole}}(Q^2) = \frac{1}{[1 + Q^2/m_D^2]^2}, \quad (4.20)$$

where

$$m_D^2 = 0.71 \text{ GeV}^2 = 18.23 \text{ fm}^{-2}. \quad (4.21)$$

Deviations of $G_E^p(Q^2)$ from the dipole formula (4.20) have indeed been reported for $Q^2 \lesssim 5 \text{ fm}^{-2}$ (cf. [53] and references cited therein). We leave quantitative fits of these effects with our ansatz to further work.

If we apply the same exclusive-inclusive argument used above for the nucleons to the electromagnetic formfactor of the pion we seem to run into a problem: The electromagnetic formfactor of the π^0 is strictly zero due to current conservation and CPT invariance. On the other hand, the inclusive synchrotron photon radiation from a π^0 is nonzero since the structure function $F_2^\pi(x)$ is nonzero (cf. the analogue of (2.29) for a π^0). We can resolve this paradox in a way suggested a long time ago for the analogous case of deep inelastic scattering by assuming that the transition formfactor $\pi \rightarrow \rho$ in

$$\pi^0(p) \rightarrow \rho^0(p') + \gamma(q) \quad (4.22)$$

in reactions analogous to those of Fig. 8 has a piece dual to synchrotron radiation. Thus we predict the presence of “anomalous” terms $\propto (Q^2)^{1/6}$ in the formfactors for (4.22). The π^0 formfactor being zero and thus having certainly no “anomalous” piece it would seem natural to us that also the charged pion formfactor has no “anomalous” piece.

5 Conclusions

In this article we have argued that the nontrivial vacuum structure in QCD should lead to the emission of soft photons in addition to hadronic bremsstrahlung in hadron-hadron collisions. We compared our theoretical results with the data from proton-Beryllium scattering at 450 GeV incident proton momentum [3]. We found that the data does indeed allow for a contribution from “synchrotron” photons. We obtained a decent description of the data adding the photon spectra from hadronic bremsstrahlung and from our “synchrotron” effect (3.4) with an effective length $l_{\text{eff}} \simeq 20 \text{ fm}$. The physical meaning of l_{eff} is explained in Fig. 3. Inserting this in (2.28) and using for the

mean transverse momentum of quarks in a hadron $\sigma = 300 \text{ MeV}$ (cf. (2.33)) leads to an effective field strength

$$gB_c = \frac{\sigma}{l_{\text{eff}}} \simeq (55 \text{ MeV})^2. \quad (5.1)$$

This is much smaller than the vacuum field strength (2.3) deduced from the QCD sum rules. We must conclude that quarks in a *fast moving* hadron see only a *shielded* vacuum chromomagnetic field. This shielding is presumably done by the gluons in the hadrons. Indeed, we know from deep inelastic scattering that roughly 50% of the momentum of a fast hadron is carried by gluons. We find here a vital role to play for these gluons: shielding the vacuum colour fields. Indeed if we insert the vacuum field strength (2.3) and $\sigma = 300 \text{ MeV}$ in (2.28) we get only a tiny $l_{\text{eff}} = 0.12 \text{ fm}$! A wiggling around of quarks in a fast hadron over such tiny length scales is quite contrary to all the physical picture which emerges from deep inelastic scattering. It would, for instance, lead to large violations of the Callen-Gross relation [54] which are not observed in experiment.

We have then argued, by making an exclusive-inclusive connection, that the nucleon electromagnetic formfactors should contain terms proportional to $(Q^2)^{1/6}$ for $0 < Q^2 \lesssim 1 \text{ GeV}^2$. We found that the data for the neutron electric formfactor shows a behaviour quite consistent with this. Applying the same arguments to the pion formfactor we concluded that the electromagnetic formfactors of π^\pm should *not* contain such a $(Q^2)^{1/6}$ piece, but the $\pi \rightarrow \rho$ transition formfactor should.

Clearly the ideas presented in this article are rather speculative. However, we can now cite at least three “anomalous” effects for which we give a common interpretation in terms of the QCD vacuum structure:

- (1) the spin effects in the Drell-Yan process [20],
- (2) soft photon production in hadronic collisions,
- (3) the Q^2 behaviour of the neutron electric formfactor.

We think it should be a worthwhile goal for experimentalists to support or disprove the above theoretical ideas with more and more precise data.

Finally, let us make some general comments and pose some questions on anomalous prompt soft photons in hadron-hadron and lepton-hadron scattering.

- (1) The most important point is, of course, to establish or disprove their existence experimentally. A good place to check the presence of anomalous photons are reactions where only neutral hadrons participate, e.g.

$$\begin{aligned}K_L + n &\rightarrow K_L + n + \gamma, \\ \Lambda + n &\rightarrow \Lambda + n + \gamma.\end{aligned}\quad (5.2)$$

Then bremsstrahlung is highly suppressed since it is only due to magnetic moments of the neutral hadrons and “anomalous” photons should then be a clear signal. Experimental investigation of the reactions (5.2) is not totally hopeless. One could use K_L - or Λ -deuteron scattering with the proton as spectator. Bremsstrahlung photons from this soft proton should be reliably calculable.

- (2) Do the anomalous photons come from the particles in the initial state, in the final state or from both the initial and final state particles – or do they come from some other mechanism? The answer should be given by

the dependence of the photon yield on the hadronic multiplicity in the collision. It should also be interesting to look for correlations between hadronic energy flow and the photon emission angles. A “thermal” production mechanism as proposed e.g. in the “glob” model should produce photons in a more isotropic way than the synchrotron mechanism discussed here where the photons follow more or less the initial and final hadrons’ directions.

(3) Do the anomalous photons come from the hadrons or from the quarks in the hadrons, i.e. do the quarks in the hadrons act coherently or incoherently? It should be possible to answer this question by comparing reactions where hadrons with different charge but similar structure functions F_2 participate. Examples are

$$\begin{aligned} A + p &\rightarrow \text{hadrons}, \\ \Sigma^+ + p &\rightarrow \text{hadrons}; \end{aligned} \quad (5.3)$$

or

$$\begin{aligned} p + p &\rightarrow p + p + \text{mostly neutral pions}, \\ p + p &\rightarrow p + p + \text{mostly charged pions}. \end{aligned} \quad (5.4)$$

(4) The frequency, angular, and s -dependence of the anomalous photons should be quite revealing. In this paper we have discussed in detail the frequency and angular dependence predicted in our model. The s -dependence enters in two ways (cf. (2.40)): Through the hadronic one particle inclusive distributions and through the synchrotron formula (2.27), (2.29) and its analogues for the final state hadrons. There we have to use the structure function F_2 at some effective Q^2 . Taking the latter to increase with \sqrt{s} , as seems quite reasonable, we come sooner or later into the region $Q^2 \gtrsim 10 \text{ GeV}^2$ where HERA data [41] show a large increase of F_2 for $x \rightarrow 0$. Taking for instance the estimate (3.6) for the effective Q^2 we find $Q^2 \simeq 100 \text{ GeV}^2$ for $\sqrt{s} = 2000 \text{ GeV}$, i.e. at Tevatron energies. Thus our model – as well as all models of soft photon production where the quarks in hadrons act incoherently – will predict a substantial increase of the photon yield with c.m. energy \sqrt{s} due to the increase of the quark densities measured by F_2 .

(5) The production of soft lepton pairs, e^+e^- and $\mu^+\mu^-$ is most probably a related phenomenon since the lepton pairs surely come from virtual photons γ^* . There one has the possibility to investigate the polarization of the virtual photons γ^* by analysing the angular distributions of the lepton pairs in the γ^* rest system. Polarization phenomena could lead to sensitive tests of theoretical models.

We hope that some of our remarks above may be useful for the discussion and clarification of the intriguing phenomenon of “anomalous photons”.

Acknowledgements. The authors would like to thank H.G. Dosch, B.R. French, D. Gromes, G. Ingelman, P.V. Landshoff, F. Lenz, H. Leutwyler, P. Lichard, M. Neubert, H.J. Specht, M. Spyropoulou-Stassinaki, Th. Walcher for useful discussions and correspondence. Special thanks are due to H.J. Specht for providing the normalization of the data of [3] on prompt photons and to P.V. Landshoff and H.G. Dosch for reading the manuscript, part of which was written while one of the authors (O.N.) was visiting DAMTP of Cambridge University. This author would like to thank P.V.

Landshoff for the hospitality extended to him there and the DAAD for supporting this visit financially under project Nr. 313-ARC-VIII-vo/scu.

Appendix A

In this appendix we discuss the emission of “synchrotron” photons by two quarks of a hadron and estimate the frequency range over which the emission from two quarks can be considered as being incoherent.

Consider two quarks $q_{1,2}$ of a fast hadron as in Sect. 2, (2.6) ff. To calculate their synchrotron emission we treat the quarks as classical charged point particles moving in the background chromomagnetic vacuum field (cf. [2]). Let the world lines of q_1 and q_2 be parametrized by the times t_i :

$$z_i(t_i) = \begin{pmatrix} t_i \\ \mathbf{z}_i(t_i) \end{pmatrix}, \quad i = 1, 2. \quad (A.1)$$

Consider first quark q_1 which moves in 3-space along the curve \mathcal{C}_1

$$\mathcal{C}_1: t_1 \rightarrow \mathbf{z}_1(t_1). \quad (A.2)$$

For all times t_1 we can construct the tangent vector \mathcal{T}_1 and the vector \mathcal{N}_1 pointing from $\mathbf{z}_1(t_1)$ to the center of the instantaneous curvature circle. The standard formulae of differential geometry (cf. e.g. [55]) give:

$$\begin{aligned} \mathcal{T}_1(t_1) &= \frac{\dot{\mathbf{z}}_1(t_1)}{|\dot{\mathbf{z}}_1(t_1)|}, \\ \mathcal{N}_1(t_1) &= \frac{1}{|\dot{\mathbf{z}}_1(t_1)|} \frac{d\mathcal{T}_1(t_1)}{dt_1}. \end{aligned} \quad (A.3)$$

The radius of curvature of \mathcal{C}_1 at the point corresponding to the time t_1 is then

$$\rho_1(t_1) = (|\mathcal{N}_1(t_1)|)^{-1}. \quad (A.4)$$

For a quark q_1 with Lorentz factor $\gamma_1(t_1)$ we can define the instantaneous cyclotron frequency and effective colour magnetic field by

$$\omega_c^1(t_1) := \frac{\sqrt{(\gamma_1(t_1))^2 - 1}}{\rho_1(t_1)}, \quad (A.5)$$

$$gB_c^1(t_1) := m_q \omega_c^1(t_1). \quad (A.6)$$

The next step is to construct the analogous quantities for quark q_2 .

The amplitude for emission of a photon of wave vector \mathbf{k} , frequency $\omega = |\mathbf{k}|$ and polarization vector $\boldsymbol{\varepsilon}$ ($\boldsymbol{\varepsilon} \cdot \mathbf{k} = 0$) by the two quarks is given by (cf. e.g. [56]):

$$A(\mathbf{k}, \boldsymbol{\varepsilon}) = ie\boldsymbol{\varepsilon}^* \mathbf{Z}(\mathbf{k}), \quad (A.7)$$

where

$$\begin{aligned} \mathbf{Z}(\mathbf{k}) &= \sum_{i=1}^2 \mathbf{Z}_i(\mathbf{k}), \\ \mathbf{Z}_i(\mathbf{k}) &= \int_{-\infty}^{\infty} dt_i \frac{d\mathbf{z}_i}{dt_i}(t_i) e^{i(\omega t_i - \mathbf{k} \cdot \mathbf{z}_i(t_i))}, \quad i = 1, 2. \end{aligned} \quad (A.8)$$

The synchrotron formulae are obtained by expanding the integrand in (A.8) around the time t_i where

$$\mathbf{k} \cdot \mathcal{N}_i(t_i) = 0. \quad (\text{A.9})$$

Let $t_{i,0}$ be the times where (A.9) is satisfied and assume that there is just one solution of (A.9) for $i = 1$ and $i = 2$. Set furthermore

$$\cos \mathcal{G}_i := \hat{\mathbf{k}} \cdot \mathcal{T}_i(t_{i,0}),$$

$$\eta_i := \frac{(t_i - t_{i,0})\omega_c^{i,0}}{(1 + \gamma_{i,0}^2 \mathcal{G}_i^2)^{1/2}}$$

$$\xi_i := \frac{\omega}{3\gamma_{i,0}^2 \omega_c^{i,0}} (1 + \gamma_{i,0}^2 \mathcal{G}_i^2)^{3/2}, \quad (\text{A.10})$$

where an index 0 indicates that the quantities are to be taken at $t_i = t_{i,0}$. We get then (cf. [56], [21]):

$$\begin{aligned} \mathbf{Z}_i(\mathbf{k}) = & \exp(i\omega t_{i,0} - i\mathbf{k}\mathbf{z}_{i,0}) \int_{-\infty}^{\infty} d\eta_i \frac{(1 + \gamma_{i,0}^2 \mathcal{G}_i^2)^{1/2}}{\omega_c^{i,0}} \\ & \times \left\{ \dot{\mathbf{z}}_{i,0} + \frac{(1 + \gamma_{i,0}^2 \mathcal{G}_i^2)^{1/2}}{\omega_c^{i,0}} \eta_i \ddot{\mathbf{z}}_{i,0} \right\} \exp \left[\frac{3}{2} \xi_i \left(\eta_i + \frac{1}{3} \eta_i^3 \right) \right], \end{aligned} \quad (\text{A.11})$$

$$\begin{aligned} \mathbf{Z}_i(\mathbf{k}) = & \frac{2}{\sqrt{3}} \frac{(1 + \gamma_{i,0}^2 \mathcal{G}_i^2)^{1/2}}{\omega_c^{i,0}} \exp(i\omega t_{i,0} - i\mathbf{k}\mathbf{z}_{i,0}) \\ & \times \left\{ \dot{\mathbf{z}}_{i,0} K_{1/3}(\xi_i) + i \frac{(1 + \gamma_{i,0}^2 \mathcal{G}_i^2)^{1/2}}{\omega_c^{i,0}} \ddot{\mathbf{z}}_{i,0} K_{2/3}(\xi_i) \right\}, \end{aligned} \quad (\text{A.12})$$

where $K_{1/3, 2/3}$ are modified Bessel functions.

The probability of photon emission is given by

$$\begin{aligned} \omega \frac{d^3 n}{d^3 k} = & \frac{\alpha}{4\pi^2} \sum_{\gamma=\text{pol.}} |\boldsymbol{\varepsilon}^* \cdot \mathbf{Z}(\mathbf{k})|^2 \\ = & \frac{\alpha}{4\pi^2} (|\mathbf{Z}(\mathbf{k})|^2 - |\hat{\mathbf{k}} \cdot \mathbf{Z}(\mathbf{k})|^2). \end{aligned} \quad (\text{A.13})$$

The angular width of the photon distribution is estimated by $\xi_i \lesssim 1$, since the Bessel functions $K_{1/3, 3/2}(\xi_i)$ drop exponentially for $\xi_i > 1$.

Suppressing here indices $i, 0$ we get from (A.10):

$$\xi \lesssim 1 \Rightarrow \mathcal{G}^2 \lesssim \left(\frac{3}{\gamma} \frac{\omega_c}{\omega} \right)^{2/3} =: \mathcal{G}_{\max}^2. \quad (\text{A.14})$$

As to be expected, the emission occurs for small \mathcal{G} , i.e. in a narrow cone around the velocity vectors $\dot{\mathbf{z}}_{i,0}$ for large γ . According to (A.11) the radiation is obtained from small time intervals Δt around the times $t_{i,0}$. We can estimate Δt from the condition $|\eta_i| \lesssim 1$. This gives, taking into account (A.14):

$$\begin{aligned} \frac{\Delta t \omega_c}{(1 + \gamma^2 \mathcal{G}^2)^{1/2}} & \simeq 1, \\ \Rightarrow \Delta t \omega_c \left(3\gamma^2 \frac{\omega_c}{\omega} \right)^{-1/3} & \simeq 1, \\ \Rightarrow \Delta t & \simeq (3\gamma^2)^{1/3} \omega_c^{-2/3} \omega^{-1/3}. \end{aligned} \quad (\text{A.15})$$

Another way to arrive at (A.15) is to calculate the time $\Delta t'$ over which the velocity vector of the quark moving

approximately on a circle of radius ρ (A.4) points inside a cone of angle $\mathcal{G} \leq \mathcal{G}_{\max}$ around \mathbf{k} . Indeed, we find from (A.4), (A.5) and (A.14)

$$\Delta t' \simeq \rho \cdot \mathcal{G}_{\max} = \frac{\gamma}{\omega_c} \left(\frac{3}{\gamma} \frac{\omega_c}{\omega} \right)^{1/3} \equiv \Delta t. \quad (\text{A.16})$$

Consider first quarks being almost “wee”. We have then from (2.20)

$$\gamma = E_{\text{wee}}^{\max}/m_q = \frac{1}{am_q}, \quad (\text{A.17})$$

$$\begin{aligned} \Delta t & \simeq \left(\frac{1}{am_q} \right)^{2/3} \left(\frac{gB_c}{m_q} \right)^{-2/3} \omega^{-1/3} \\ & = \left(\frac{1}{agB_c} \right)^{2/3} \omega^{-1/3} \\ & = \left(\frac{l_{\text{eff}}}{a\sigma} \right)^{2/3} \omega^{-1/3}. \end{aligned} \quad (\text{A.18})$$

Coherence effects between the emission from quarks q_1 and q_2 should certainly show up if the integration length (A.18) exceeds the time interval Δt_0 (2.21) for which q_1 and q_2 can be considered as moving in uncorrelated background fields:

$$\Delta t \gtrsim \Delta t_0,$$

$$\Rightarrow \omega \lesssim m_q \left(\frac{m_q}{\sigma} \right)^2 \left(\frac{l_{\text{eff}}}{R} \right)^2 \frac{a}{R} =: \bar{\omega} \quad (\text{A.19})$$

With $m_q = 10$ MeV, $\sigma = 300$ MeV, $a = 0.35$ fm, $R = 1$ fm, and $l_{\text{eff}} = 30$ fm this leads to

$$\bar{\omega} = 3.5 \text{ MeV}. \quad (\text{A.20})$$

For $\omega \gtrsim \bar{\omega}$ on the other hand we have $\Delta t \lesssim \Delta t_0$ and the almost wee quarks q_1 and q_2 travel during the emission in uncorrelated colour domains. For “harder” quarks q_1, q_2 this is true a fortiori since $\Delta t(x_1)$ defined in (2.19) grows proportional to γ (cf. (2.18)) whereas Δt of (A.15) is only proportional to $\gamma^{2/3}$. The emission rate (A.13) is determined by

$$\begin{aligned} |\boldsymbol{\varepsilon}^* \mathbf{Z}(\mathbf{k})|^2 = & |\boldsymbol{\varepsilon}^* \mathbf{Z}_1(\mathbf{k}) + \boldsymbol{\varepsilon}^* \mathbf{Z}_2(\mathbf{k})|^2 \\ = & |\boldsymbol{\varepsilon}^* \mathbf{Z}_1(\mathbf{k})|^2 + |\boldsymbol{\varepsilon}^* \mathbf{Z}_2(\mathbf{k})|^2 + 2\text{Re}[(\boldsymbol{\varepsilon}^* \mathbf{Z}_1(\mathbf{k}))(\boldsymbol{\varepsilon} \cdot \mathbf{Z}_2^*(\mathbf{k}))]. \end{aligned} \quad (\text{A.21})$$

Looking at (A.12) we see that the 1–2 interference term on the r.h.s. of (A.21) is proportional to $\boldsymbol{\varepsilon}^* \dot{\mathbf{z}}_{1,0}, \boldsymbol{\varepsilon}^* \ddot{\mathbf{z}}_{1,0}$ multiplied by $\boldsymbol{\varepsilon} \dot{\mathbf{z}}_{2,0}, \boldsymbol{\varepsilon} \ddot{\mathbf{z}}_{2,0}$. But in the case we are considering these transverse (with respect to \mathbf{k}) velocities and accelerations of the quarks q_1, q_2 at the times $t_{1,0}, t_{2,0}$ are uncorrelated. In a sum over histories which we have to perform in (A.21) the interference term should, therefore, vanish.

To summarize: In this appendix we have given arguments that for $\omega \gtrsim \bar{\omega}$ (A.20) the emission of synchrotron photons from quarks in a hadron can be added incoherently while for $\omega \lesssim \bar{\omega}$ coherence effects will be important. We have worked here in a fixed reference frame where the hadron and its quarks move reasonably fast. The angles of the quark velocity vectors relative to the hadron’s velocity

vector will vary from zero up to angles of the order $\sigma/E_{\text{wee}}^{\text{max}} \simeq \sigma a = \mathcal{O}(1)$. The emission angles of the synchrotron photons with respect to the hadron's velocity vary then also up to angles of order 1 and the coherence condition $\omega \lesssim \bar{\omega}$ implies then

$$|\mathbf{k}_T| \lesssim \bar{\omega} \quad (\text{A.22})$$

where \mathbf{k}_T is transverse with respect to the hadron's velocity vector.

To obtain the results from [2] we still have to average over all suitable reference frames obtained by a boost along the collision axis from the c.m. system. Since \mathbf{k}_T is invariant under such boosts we would then expect from (A.22) to see coherence for photon transverse (with respect to the collision axis) momenta:

$$|\mathbf{k}_T| \lesssim \bar{\omega} \quad (\text{A.23})$$

and incoherence for

$$|\mathbf{k}_T| \gtrsim \bar{\omega}. \quad (\text{A.24})$$

Of course, (A.23), (A.24) should be considered only as *rough* guides for the regions of coherence and incoherence.

Appendix B

In this appendix we discuss a simple model in order to make clear what is meant by “dressed” and “naked” hadrons and by the symbolic equations (2.35) and (2.36).

Consider a model with two scalar hermitean fields: a field $\psi(x)$ of mass m and a zero mass field $\varphi(x)$. As Lagrangian we choose:

$$L(t) = \int d^3x \frac{1}{2} \{ \partial_\mu \psi(x) \partial^\mu \psi(x) - m^2 \psi^2(x) + \partial_\mu \varphi(x) \partial^\mu \varphi(x) + 2g\psi^2(x)\varphi(x) - 2\psi^2(x)V(\mathbf{x}) \}, \quad x = (t, \mathbf{x}). \quad (\text{B.1})$$

The field ψ is the analogue of the quark and hadron fields, the static potential $V(\mathbf{x})$ represents the strong interaction, φ and g are the analogues of the photon field and the electromagnetic coupling, respectively.

We want to study the reactions

$$\begin{aligned} \text{(a)} \quad & \psi(\mathbf{p}) \rightarrow \psi(\mathbf{p}'), \\ \text{(b)} \quad & \psi(\mathbf{p}) \rightarrow \psi(\mathbf{p}') + \varphi(\mathbf{k}), \end{aligned} \quad (\text{B.2})$$

where for simplicity we work only up to first order in the coupling constant g and the potential V .

The Feynman rules following from (B.1) are shown in Fig. 11, where

$$\tilde{V}(\mathbf{q}) := \int d^3x e^{-i\mathbf{q}\cdot\mathbf{x}} V(\mathbf{x}). \quad (\text{B.3})$$

The diagrams for the reactions (a), (b) of (B.2) are shown in Fig. 12. They lead to the following S -matrix elements:

$$\langle \psi(\mathbf{p}') | S | \psi(\mathbf{p}) \rangle = -4i\pi\delta(p'^0 - p^0) \tilde{V}(\mathbf{p}' - \mathbf{p}), \quad (\text{B.4})$$

$$\begin{aligned} \langle \psi(\mathbf{p}') \varphi(\mathbf{k}) | S | \psi(\mathbf{p}) \rangle &= 8\pi i g \delta(p'^0 + \omega - p^0) \\ &\times \tilde{V}(\mathbf{p}' + \mathbf{k} - \mathbf{p}) \left[-\frac{1}{2pk} + \frac{1}{2p'k} \right], \end{aligned} \quad (\text{B.5})$$

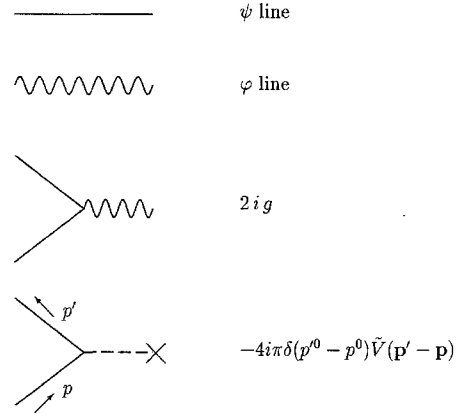


Fig. 11. Feynman rules following from the Lagrangian (B.1)

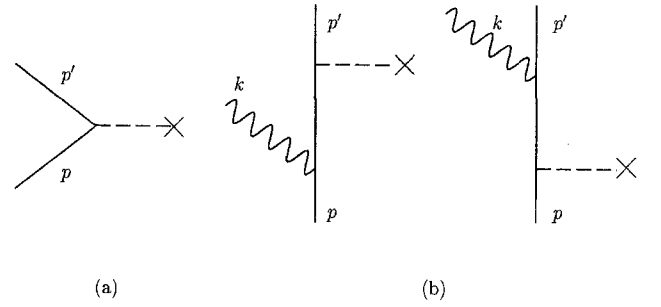


Fig. 12. Lowest order diagrams for the reactions (a) and (b) of (B.2)

where $\omega \equiv k^0$. The cross sections for reactions (a), (b) of (B.2) are

$$\frac{d\sigma^{(a)}}{d\Omega'} = \frac{1}{16\pi^2} |2\tilde{V}(\mathbf{q})|^2, \quad (\text{B.6})$$

$$\frac{\omega d\sigma^{(b)}}{d\Omega' d^3k} = \frac{|\mathbf{p}'|}{|\mathbf{p}| 16\pi^2} |2\tilde{V}(\mathbf{q} + \mathbf{k})|^2 \frac{2g^2}{(2\pi)^3} \left| \frac{1}{2pk} - \frac{1}{2p'k} \right|^2, \quad (\text{B.7})$$

where $\mathbf{q} := \mathbf{p}' - \mathbf{p}$ and $d\Omega'$ is the solid angle element corresponding to \mathbf{p}' . All this is, of course, completely standard.

Now we will rederive these formulae using “old-fashioned” methods, i.e. in the Hamiltonian approach (cf. e.g. [57]). From the Lagrangian (B.1) we find the canonical momenta conjugate to $\psi(x)$ and $\varphi(x)$ as

$$\begin{aligned} \Pi_\psi(x) &= \dot{\psi}(x), \\ \Pi_\varphi(x) &= \dot{\varphi}(x) \end{aligned} \quad (\text{B.8})$$

and the Hamiltonian

$$H(t) = H_0(t) + H_g(t) + H'(t) \quad (\text{B.9})$$

where

$$\begin{aligned} H_0(t) &= \int d^3x \frac{1}{2} [(\Pi_\psi(x))^2 + (\nabla\psi(x))^2 + m^2\psi^2(x) \\ &\quad + (\Pi_\varphi(x))^2 + (\nabla\varphi(x))^2], \\ H_g(t) &= -g \int d^3x \psi^2(x) \varphi(x), \\ H'(t) &= \int d^3x \psi^2(x) V(\mathbf{x}). \end{aligned} \quad (\text{B.10})$$

We work now in the Schrödinger representation, setting $t = 0$ in the dynamical variables and in the Hamiltonian,

$$\psi(\mathbf{x}) \equiv \psi(0, \mathbf{x}),$$

$$H \equiv H(0), \text{ etc.} \quad (\text{B.11})$$

We then impose the canonical commutation relations for ψ , Π_ψ and φ , Π_φ and expand these field operators in terms of annihilation and creation operators (cf. chapter 3 of [13] for all conventions concerning normalizations). Let us denote by $b(\mathbf{p})$ ($b^\dagger(\mathbf{p})$) the annihilation (creation) operators for ψ , Π_ψ and by $a(\mathbf{k})$ ($a^\dagger(\mathbf{k})$) those for φ , Π_φ . The next step is to expand H_0 , H_g , H' in terms of these operators and to normal order them. We get:

$$H_0 = \int \frac{d^3k}{(2\pi)^3 2\omega} \omega a^\dagger(\mathbf{k}) a(\mathbf{k})$$

$$+ \int \frac{d^3p}{(2\pi)^3 2p^0} p^0 b^\dagger(\mathbf{p}) b(\mathbf{p}), \quad (\omega \equiv k^0), \quad (\text{B.12})$$

$$H_g = -g \int \frac{d^3p' d^3p d^3k}{(2\pi)^6 2p'^0 2p^0 2\omega}$$

$$\times \{ b^\dagger(\mathbf{p}') b^\dagger(\mathbf{p}) [\delta^{(3)}(\mathbf{p}' + \mathbf{p} + \mathbf{k}) a^\dagger(\mathbf{k})$$

$$+ \delta^{(3)}(\mathbf{p}' + \mathbf{p} - \mathbf{k}) a(\mathbf{k})]$$

$$+ 2b^\dagger(\mathbf{p}') b(\mathbf{p}) [\delta^{(3)}(\mathbf{p}' - \mathbf{p} + \mathbf{k}) a^\dagger(\mathbf{k})$$

$$+ \delta^{(3)}(\mathbf{p}' - \mathbf{p} - \mathbf{k}) a(\mathbf{k})]$$

$$+ b(\mathbf{p}') b(\mathbf{p}) [\delta^{(3)}(\mathbf{p}' + \mathbf{p} - \mathbf{k}) a^\dagger(\mathbf{k})$$

$$+ \delta^{(3)}(\mathbf{p}' + \mathbf{p} + \mathbf{k}) a(\mathbf{k})] \}, \quad (\text{B.13})$$

$$H' = \int \frac{d^3p' d^3p}{(2\pi)^6 2p'^0 2p^0} \{ b^\dagger(\mathbf{p}') b^\dagger(\mathbf{p}) \tilde{V}(\mathbf{p}' + \mathbf{p})$$

$$+ 2b^\dagger(\mathbf{p}') b(\mathbf{p}) \tilde{V}(\mathbf{p}' - \mathbf{p}) + b(\mathbf{p}') b(\mathbf{p}) \tilde{V}(-\mathbf{p}' - \mathbf{p}) \}. \quad (\text{B.14})$$

We define now the “naked” states to be the eigenstates of H_0 and denote them by round brackets |):

Naked vacuum: |0)

$$a(\mathbf{k})|0) = 0,$$

$$b(\mathbf{p})|0) = 0, \quad (\text{B.15})$$

for all \mathbf{k} , \mathbf{p} . It follows:

$$H_0|0) = 0. \quad (\text{B.16})$$

Naked one-particle states:

$$|\psi(\mathbf{p})\rangle = b^\dagger(\mathbf{p})|0),$$

$$|\varphi(\mathbf{k})\rangle = a^\dagger(\mathbf{k})|0); \quad (\text{B.17})$$

$$H_0|\psi(\mathbf{p})\rangle = p^0|\psi(\mathbf{p})\rangle,$$

$$H_0|\varphi(\mathbf{k})\rangle = \omega|\varphi(\mathbf{k})\rangle. \quad (\text{B.18})$$

Our next task is to construct the eigenstates of $H_0 + H_g$. Denoting these states by the brackets | \rangle we get

in perturbation theory up to first order in g for the one- ψ -particle states:

$$|\psi(\mathbf{p})\rangle = |\psi(\mathbf{p})\rangle + g|\psi\varphi; \mathbf{p}\rangle + g|\psi^3\varphi; \mathbf{p}\rangle, \quad (\text{B.19})$$

where

$$|\psi\varphi; \mathbf{p}\rangle = 2 \int \frac{d^3k}{(2\pi)^3 2\omega} \frac{1}{2p_1^0} \frac{1}{p_1^0 + \omega - p^0} |\psi(\mathbf{p}_1)\varphi(\mathbf{k})\rangle,$$

$$\mathbf{p}_1 = \mathbf{p} - \mathbf{k}, \quad (\text{B.20})$$

and $|\psi^3\varphi; \mathbf{p}\rangle$ is a state with 3 naked ψ and one naked φ particles. The “cloud” of naked φ particles in a “physical” ψ state is given by the admixtures $|\psi\varphi; \mathbf{p}\rangle$ and $|\psi^3\varphi; \mathbf{p}\rangle$ in (B.19). The φ -particle density is defined as

$$\frac{\omega dn(\mathbf{k}; \mathbf{p})}{d^3k} = \frac{\langle \psi(\mathbf{p}) | \frac{a^\dagger(\mathbf{k}) a(\mathbf{k})}{2(2\pi)^3} | \psi(\mathbf{p}) \rangle}{\langle \psi(\mathbf{p}) | \psi(\mathbf{p}) \rangle}. \quad (\text{B.21})$$

In the following we will consider the high energy limit in reactions (a), (b) of (B.2), to be precise we require

$$p'^0, p^0 \gg m, \omega. \quad (\text{B.22})$$

In this limit the contribution $|\psi^3\varphi; \mathbf{p}\rangle$ in (B.19) can be neglected. It leads to a Z-diagram in the reaction (b) of (B.2) being suppressed by $1/p^0$ relative to the leading term. We get then for the density (B.21)

$$\frac{\omega dn(\mathbf{k}; \mathbf{p})}{d^3k} \simeq \frac{2g^2}{(2\pi)^3} \left| \frac{1}{2(pk)} \right|^2. \quad (\text{B.23})$$

Consider now the following scattering reaction induced by the Hamiltonian H' (B.14):

$$|i\rangle \rightarrow |f\rangle \quad (\text{B.24})$$

where $|i\rangle$ and $|f\rangle$ are eigenstates of $H_0 + H_g$ with energies E_i , E_f . In first Born approximation we have

$$\langle f | S | i \rangle = \delta_{fi} - 2\pi i \delta(E_f - E_i) \langle f | H' | i \rangle. \quad (\text{B.25})$$

For the reactions (B.2) we have to take for $|i\rangle$ the state $|\psi(\mathbf{p})\rangle$ (B.19). Applying H' (B.14) to it we get:

$$H'|\psi(\mathbf{p})\rangle = \int \frac{d^3p_2}{(2\pi)^3 2p_2^0} 2\tilde{V}(\mathbf{p}_2 - \mathbf{p}) |\psi(\mathbf{p}_2)\rangle$$

$$+ 2g \int \frac{d^3p_2 d^3k}{(2\pi)^6 2p_2^0 2\omega} \frac{2\tilde{V}(\mathbf{p}_2 + \mathbf{k} - \mathbf{p})}{2p_1^0(p_1^0 + \omega - p^0)} |\psi(\mathbf{p}_2)\varphi(\mathbf{k})\rangle + \dots \quad (\text{B.26})$$

Here the dots stand for terms which do not contribute to the scattering reactions (B.2) due to energy conservation and/or particle content and for terms which give vanishing contribution in the limit (B.22). The interpretation of (B.26) is clear. The action of H' scatters the naked ψ particle out of the physical one and produces a superposition of states with one naked ψ particle ($|\psi(\mathbf{p}_2)\rangle$) and one naked ψ and one φ particle ($|\psi(\mathbf{p}_2)\varphi(\mathbf{k})\rangle$). Now we reexpress these naked particle states in terms of physical ones. Inverting (B.19) we find to order g :

$$|\psi(\mathbf{p}_2)\rangle = |\psi(\mathbf{p}_2)\rangle - g|\psi\varphi; \mathbf{p}_2\rangle - g|\psi^3\varphi; \mathbf{p}_2\rangle. \quad (\text{B.27})$$

Inserting this in (B.26) and neglecting again all terms which vanish in the limit (B.22) leads to

$$\begin{aligned} H'|\psi(\mathbf{p})\rangle &= \int \frac{d^3 p_2}{(2\pi)^3 2p_2^0} 2\tilde{V}(\mathbf{p}_2 - \mathbf{p})|\psi(\mathbf{p}_2)\rangle \\ &- g \int \frac{d^3 p_2}{(2\pi)^3 2p_2^0} 2\tilde{V}(\mathbf{p}_2 - \mathbf{p})|\psi\varphi; \mathbf{p}_2\rangle \\ &+ 2g \int \frac{d^3 p_2 d^3 k}{(2\pi)^6 2p_2^0 2\omega} \frac{2\tilde{V}(\mathbf{p}_2 + \mathbf{k} - \mathbf{p})}{2p_1^0(p_1^0 + \omega - p^0)} |\psi(\mathbf{p}_2)\varphi(\mathbf{k})\rangle + \dots \end{aligned} \quad (\text{B.28})$$

The S -matrix elements for the reactions (a), (b) of (B.2) are now easily obtained from (B.25) and (B.28). For reaction (a) of (B.2) only the first term on the r.h.s. of (B.28) contributes and gives for the S -matrix element just the expression in (B.4). For reaction (b) of (B.2) we get two contributions in the S -matrix element:

$$\begin{aligned} \langle \psi(\mathbf{p}')\varphi(\mathbf{k})|S|\psi(\mathbf{p})\rangle &= -2\pi i \delta(p'^0 + \omega - p^0) \\ &\times [A(\mathbf{p}', \mathbf{k}; \mathbf{p}) + A'(\mathbf{p}', \mathbf{k}; \mathbf{p})], \end{aligned} \quad (\text{B.29})$$

where

$$\begin{aligned} A(\mathbf{p}', \mathbf{k}; \mathbf{p}) &= \frac{4g\tilde{V}(\mathbf{p}' + \mathbf{k} - \mathbf{p})}{2p_1^0(p_1^0 + \omega - p^0)} \simeq \frac{4g\tilde{V}(\mathbf{p}' + \mathbf{k} - \mathbf{p})}{2pk}, \\ A'(\mathbf{p}', \mathbf{k}; \mathbf{p}) &= -\frac{4g\tilde{V}(\mathbf{p}' + \mathbf{k} - \mathbf{p})}{2p_1^0(p'^0 + \omega - p'^0)} \\ &\simeq -\frac{4g\tilde{V}(\mathbf{p}' + \mathbf{k} - \mathbf{p})}{2p_1 k}, \quad \mathbf{p}'_1 = \mathbf{p}' + \mathbf{k}. \end{aligned} \quad (\text{B.30})$$

The amplitude A in (B.29) arises from the third term on the r.h.s. of (B.28). It represents the emission of φ particles due to the kicking out of the naked ψ particle from the original state $|\psi\rangle$ in the scattering process. The amplitude A' in (B.29) arises from the second term on the r.h.s. of (B.28). It represents the emission of φ -particles due to the “dressing” of the kicked-out naked ψ particle in the final state.

In the high energy limit (B.22) the expression for the S -matrix element (B.29) goes over into (B.5), derived from the Feynman rules. Of course, we get exactly the Feynman rules result with the Hamiltonian method if we do not make the high energy approximation.

Let us now consider a potential $V(\mathbf{x})$ of extension Δx . We expect then the typical momentum transfer \mathbf{q} to be of order

$$|\mathbf{q}| \sim \frac{1}{\Delta x}. \quad (\text{B.31})$$

Furthermore we require \mathbf{k} to be such that in the cross section (B.7) the interference term between the two terms $(2pk)^{-1}$ and $(2p'k)^{-1}$, i.e. the two amplitudes A, A' of (B.29) is negligible and that

$$\tilde{V}(\mathbf{q} + \mathbf{k}) \simeq \tilde{V}(\mathbf{q}). \quad (\text{B.32})$$

This requires

$$\begin{aligned} |\mathbf{q}|^2 &\gg m^2 + \omega^2, \\ \omega &\ll \frac{1}{|\mathbf{q}|\Delta x^2}. \end{aligned} \quad (\text{B.33})$$

We get then for the cross section of reaction (b) of (B.2) in the limit (B.22) :

$$\frac{\omega d\sigma^{(b)}}{d\Omega' d^3 k} \simeq \frac{d\sigma^{(a)}}{d\Omega'} \left\{ \frac{\omega dn(\mathbf{k}; \mathbf{p})}{d^3 k} + \frac{\omega dn(\mathbf{k}; \mathbf{p}')}{d^3 k} \right\}. \quad (\text{B.34})$$

The total number density of φ particles produced in the reaction (b) of (B.2)

$$\frac{\omega dn_{\text{tot}}(\mathbf{k})}{d^3 k} := \frac{\omega d\sigma^{(b)}}{d\Omega' d^3 k} \bigg/ \frac{d\sigma^{(a)}}{d\Omega'} \quad (\text{B.35})$$

is thus given by the sum of the densities of “naked” φ particles in the original and in the scattered ψ particles. We have made the analogous assumption for our synchrotron effect in (2.39), (2.40). Of course, the number densities (B.23), (B.35) in our model are proportional to ω^{-2} corresponding to bremsstrahlung, whereas for the synchrotron effect we derived a behaviour proportional to $\omega^{-4/3}$. But this should not spoil the general argument. For sake of orientation, let us finally use the estimates (B.33) for the case of hadron-hadron scattering. Then we would identify ψ with the quark field and set

$$\Delta x \simeq a \quad (\text{B.36})$$

where a is the correlation length (2.4). The typical momentum transfers should then satisfy

$$|\mathbf{q}| \lesssim 1/a = 570 \text{ MeV} \quad (\text{B.37})$$

and from (B.33) we find that for (B.34) to hold we should require for ω :

$$\omega^2 + m_q^2 \ll |\mathbf{q}|^2, \quad (\text{B.38})$$

$$\omega \ll \frac{1}{|\mathbf{q}|\Delta x^2} \simeq \frac{1}{a} = 570 \text{ MeV}. \quad (\text{B.39})$$

For light quarks with $m_q \simeq 10 \text{ MeV}$ both (B.38) and (B.39) are satisfied for $\omega \lesssim 200 \text{ MeV}$ which is very reasonable and agrees with the estimates which were made in [2].

To conclude: In this appendix we have studied a model where we could give a precise meaning to the “ φ cloud” of a particle, the analogue of the “ γ cloud” of a hadron, and to analogues of (2.35), (2.36), (2.39), (2.40).

References

1. F.E. Low: Phys. Rev. 110, 974 (1958)
2. O. Nachtmann, A. Reiter: Z. Phys. C24, 283 (1984)
3. J. Antos et al.: Z. Phys. C59, 547 (1993)
4. G.K. Savvidy: Phys. Lett. 71B, 133 (1977)
5. A.I. Vainshtein, V.I. Zakharov, M.A. Shifman: JETP Lett. 27, 55 (1978)
6. N.K. Nielsen, P. Olesen: Nucl. Phys. B144, 376 (1978)
7. M.A. Shifman, A.I. Vainshtein, V.I. Zakharov: Nucl. Phys. B147, 385, 448, 519 (1979)
8. G. 't Hooft: Cargèse Lectures, ed. G. 't Hooft et al., New York, London 1980; G. 't Hooft: Acta Phys. Austr. Suppl. XXII, 531 (1980)
9. G. Mack: Acta Phys. Austr. Suppl. XXII, 509 (1980)
10. J. Ambjørn, P. Olesen: Nucl. Phys. B170, 60, 265 (1980)
11. H.M. Fried, B. Müller (eds.): “QCD Vacuum Structure”, Proc. of the workshop on QCD vacuum structure and its applications, Paris 1992 (World Scientific, Singapore etc. 1993)

12. H.G. Dosch: "Nonperturbative Methods in Quantum Chromodynamics", Prog. in Part. and Nucl. Phys. 33, 121 (1994)
13. O. Nachtmann: "Elementary Particle Physics" (Springer, Berlin, Heidelberg 1990)
14. M.B. Voloshin: Nucl. Phys. B154, 365 (1979); H. Leutwyler: Phys. Lett. B98, 447 (1981); D. Gromes: Phys. Lett. B115, 482 (1982)
15. V.N. Baier, Yu.F. Pinelis: Phys. Lett. B116, 179 (1982)
16. P.V. Landshoff, O. Nachtmann: Z. Phys. C35, 405 (1987)
17. H.G. Dosch: Phys. Lett. B190, 177 (1987); Yu.A. Simonov: Yad. Fiz. 48, 1381 (1988), 50, 213 (1989); H.G. Dosch, Yu.A. Simonov: Phys. Lett. B205, 339 (1988)
18. H.G. Dosch, E. Ferreira, A. Krämer: Phys. Rev. D50, 1992 (1994)
19. J. Gasser, H. Leutwyler: Phys. Rep. C87, 77 (1982)
20. A. Brandenburg, E. Mirkes, O. Nachtmann: Z. Phys. C60, 697 (1993)
21. J.D. Jackson: Rev. Mod. Phys. 48, 417 (1976)
22. B. Andersson, G. Gustafson, G. Ingelman, T. Sjöstrand: Phys. Rep. C97, 33 (1983)
23. A. Messiah: "Mécanique Quantique" (Dunod, Paris, 1959, 1964)
24. R. Rückl: "Weiche elektromagnetische Bremsstrahlung in hadronischen Vielteilchen-Reaktionen", Dissertation, Univ. München (1976)
25. A.T. Goshaw et al.: Phys. Rev. Lett. 43, 1065 (1979)
26. P.V. Chliapnikow et al.: Phys. Lett. B141, 276 (1984)
27. F. Botterweck et al.: Z. Phys. C51, 541 (1991)
28. S. Abatzis et al.: Nucl. Phys. A525, 487c (1991)
29. S. Banerjee et al.: Phys. Lett. B305, 182 (1993)
30. J.J. Aubert et al.: Phys. Lett. B218, 248 (1989)
31. P. Lichard, N. Pišútová, J. Pišút: Z. Phys. C42, 641 (1989)
32. P. Lichard, J.A. Thompson: Phys. Rev. D44, 668 (1991)
33. J.D. Bjorken, H. Weisberg: Phys. Rev. D13, 1405 (1976)
34. V. Černý, P. Lichard, J. Pišút: Phys. Lett. B70, 61 (1977), Acta Phys. Pol. B9, 901 (1978), Phys. Rev. D24, 652 (1981), Z. Phys. C31, 163 (1986)
35. L. Van Hove: Ann. Phys. (N.Y.) 192, 66 (1989)
36. P. Lichard, L. Van Hove: Phys. Lett. B245, 605 (1990)
37. G. Giacomelli, M. Jacob: Phys. Rep. C55, 1 (1979)
38. A.D. Martin, R.G. Roberts, W.J. Stirling: Phys. Lett. B306, 145 (1993)
39. O. Nachtmann: Ann. Phys. (N.Y.) 209, 436 (1991)
40. R.P. Feynman: Phys. Rev. Lett. 23, 1415 (1969); "Photon-Hadron Interactions" (W.A. Benjamin, New York and Amsterdam, 1972)
41. I. Abt et al. (H1-Coll.): Nucl. Phys. B407, 515 (1993); M. Derrick et al. (ZEUS Coll.): "Measurement of the proton structure function F_2 in ep scattering at HERA", DESY-report 93-110 (1993) (unpublished)
42. A.V. Kotwal et al. (E665 Coll.): "Structure Functions and Structure Function Ratio $F_2^{(n)}/F_2^{(p)}$ at low x and Q^2 in inelastic muon scattering", Report FERMILAB-CONF-94-251-E (1994) (unpublished)
43. P.J. Sutton, A.D. Martin, R.G. Roberts, W.J. Stirling: Phys. Rev. D 45, 2349 (1992)
44. Particle Data Group: Phys. Lett. B239, 1 (1990)
45. A.M. Rossi et al.: Nucl. Phys. B84, 269 (1975)
46. M. Bourquin, J.M. Gaillard: Nucl. Phys. B114, 334 (1976)
47. P. Lichard: "Consistency of data on soft photon production in hadronic interactions", Univ. of New York at Stony Brook report SUNY-NTG-94-41 (1994) (unpublished)
48. E. Fermi: Z. Phys. 29, 315 (1924); C.F. v. Weizsäcker: Z. Phys. 88, 612 (1934); E.J. Williams: Kgl. Danske Videnskab. Selskab. Mat.-Fiz. Medd. 13, N4 (1935)
49. V.M. Budnev et al.: Phys. Rep. C15, 181 (1975)
50. S. Platchkov et al.: Nucl. Phys. A510, 740 (1990)
51. M. Meyerhoff et al.: "First measurement of the electric form-factor of the neutron in the exclusive quasielastic scattering of polarized electrons from polarized ^3He ", Univ. Mainz report (1994)
52. H. Leeb, C. Teichtmeister: Phys. Rev. C48, 1719 (1993)
53. F. Borkowski et al.: Nucl. Phys. A222, 269 (1974), B93, 461 (1975)
54. C.G. Callen jr., D.J. Gross: Phys. Rev. Lett. 22, 156 (1969)
55. W.I. Smirnow: "Lehrgang der höheren Mathematik", Teil II, 17th ed., Dt. Verlag d. Wiss. (Berlin 1986)
56. J.D. Jackson: "Classical Electrodynamics", 2nd ed. (John Wiley, New York etc. 1962)
57. W. Heitler: "The Quantum Theory of Radiation", 3rd ed. (Oxford Univ. Press, Oxford 1954)